A REMOTELY CONTROLLED ELECTRON GUN FOR A 200 keV ELECTROSTATIC ACCELERATOR

By

Alexander H. Lipnicki

A thesis submitted in partial fulfillment of the requirements for the degree of

Bachelor of Science

Houghton College

December 2013

Signature of Author …………………………………………………………………

Department of Physics
December 1, 2013

………………………………………………………………………………………..

Dr. Mark Yuly
Professor of Physics
Research Supervisor

………………………………………………………………………………………..

Dr. Donell Brandon Hoffman
Assistant Professor of
Physics

A REMOTELY CONTROLLED ELECTRON GUN FOR A 200 keV ELECTROSTATIC ACCELERATOR

By

Alexander H. Lipnicki

Submitted to the Department of Physics
On December 1, 2013 in partial fulfillment for the degree of
Bachelor of Science

Abstract

One problem encountered in the design for the Houghton College electrostatic electron accelerator is the electron source, which must be operated while floating at a potential of 200 kV. The simple two-grid electron gun used previously did not have electrodes to provide focusing and positioning of the beam. A new electron gun was constructed using an RCA 3RP1 cathode ray tube. This electron gun may be remotely controlled via an Ethernet-GPIB-RS232-Fiber optic link to a BASIC stamp-2 microcontroller inside the high voltage terminal. This microcontroller controls the intensity, focus, and acceleration grids of the cathode ray tube using a 12-bit four channel DAC7624 digital-to-analog converter, which, after current amplification, drives four EMCO G20 DC to HV DC converters.

Thesis Supervisor: Dr. Mark Yuly

Title: Professor of Physics

TABLE OF CONTENTS

TABLE OF FIGURES

Chapter 1

INTRODUCTION AND HISTORY OF ELECTROSTATIC ACCELERATORS

1.1   Introduction

For almost a hundred years the primary tool of nuclear and particle physics has been the particle accelerator. Particle accelerators produce beams of particles with energies, intensities and types of particles that cannot be otherwise obtained. With these particle beams, experiments can be performed to investigate nuclear structure and nuclear interactions. Consequently, a 200 keV electrostatic electron accelerator, which can be used for electron scattering experiments, has been constructed at Houghton College. This accelerator will produce an electron beam, bremsstrahlung x-rays from electron impact and finally, if the electron source is replaced by an ion source, beams of ions. It may even be possible to utilize the D-D fusion reaction to create fast neutrons.

1.2   Overview of Scattering Experiments

Two of the obstacles to studying the nucleus are its small size and that it is effectively shielded by electrons. Most of the physical properties of the atom, such as chemical bonding and atomic energy levels, depend almost entirely on the electrons, and are therefore insensitive to the nucleus. For this reason, one of the most successful ways to learn about the nucleus of an atom has been scattering experiments, as shown in Figure 1. This kind of experiment has a target struck by an energetic beam of particles. The incident particles have a probability of interacting with the nuclei and being deflected.

After interacting, the outgoing and residual particles can be detected. From the resulting trajectories and energies of the particles differential cross sections can be calculated. By comparing theoretical predictions to those experimental results further theories of the nucleus are developed.
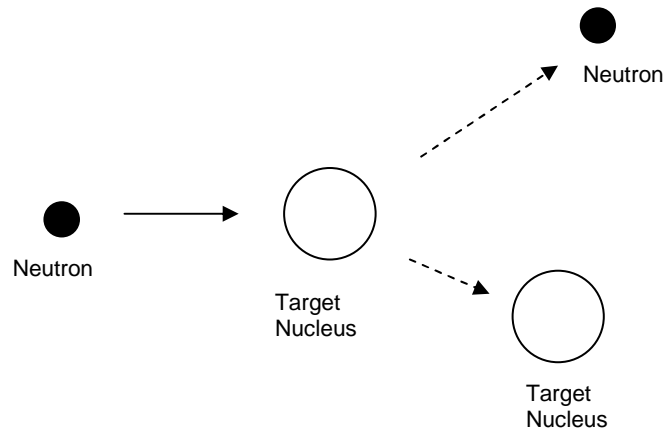
Figure 1. Example of neutron scattering. Initially the target nucleus is at rest. Neutrons with a known energy scatter from the target causing it to recoil.

1.3   Early Scattering Experiments

The most famous early experiments in nuclear physics are Ernest Rutherford's gold foil experiments [1,2] of 1909 and 1911 in which thin sheets of gold were struck by alpha particles (helium nuclei) generated by the decay of radium. The outgoing particles were detected by a scintillating zinc sulfide screen which emitted flashes of light when struck by energetic particles. Given that the mass and the momentum of the alpha particle was relatively large it was expected, especially with the extremely thin gold foil, that the particles would be deflected only very marginally given the then current "plum pudding" model of the atom which held that matter was a rather homogenous soup of positive matter and negative electrons as shown in Figure 2. However, Rutherford discovered a

small percentage of the alpha particles were ejected nearly backwards. It was described by Rutherford "as if you fired a 15-inch shell at a piece of tissue paper and it came back and hit you" [3].
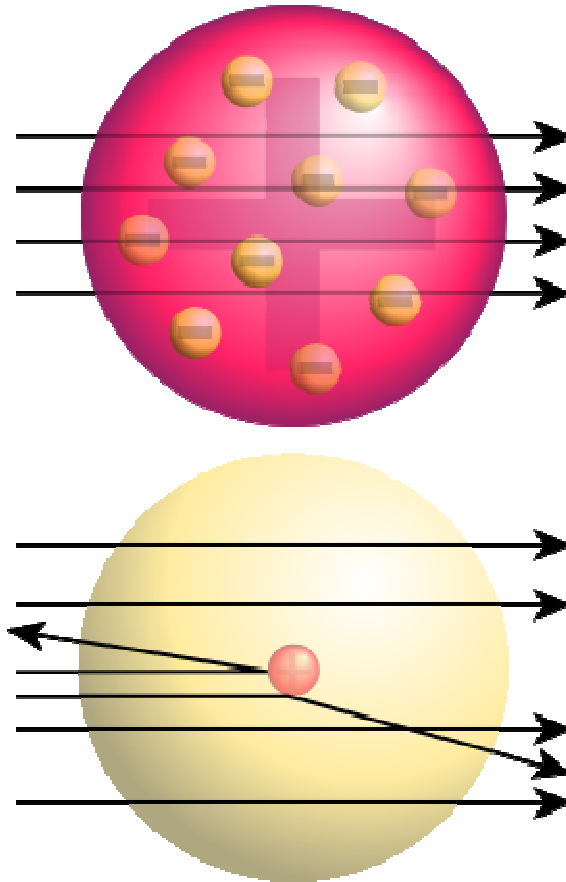
Figure 2. Comparison of plum pudding model (above) to Rutherford model (below). Rutherford expected that with the then current plum pudding model most of the incident particles would not be deflected by a sizable angle. However, some were deflected backwards leading to the development of the theory of the nucleus.

From this discovery Rutherford deduced that the nucleus of atoms contain a very small massive positive charge, surrounded by point like electrons while the rest of the atom was empty space.

1.4   Splitting the Atom

In 1919 Rutherford performed another very important experiment [4] in which he was first to split an atom apart. In this experiment he utilized a setup similar to his gold leaf experiment, with a radium alpha source and a zinc sulfide scintillating screen. The radium (^{223}Ra) ejects alpha particles with energies up to 6 MeV. Upon the introduction of nitrogen gas the number of scintillations was seen to increase rather than decrease as expected due to the nitrogen gas acting to block alpha particles. Therefore, Rutherford theorized that the alpha particles broke the nitrogen nuclei apart. This was surprising, since it meant the energy required to penetrate to the nucleus was less than originally thought [4]. This effect was later recognized to be due to quantum mechanical tunneling [5].

Radioactive sources only allowed for certain discrete energies and types of particles to be used. Rutherford in 1927 declared [6] that he hoped that energies beyond those available by natural sources would be someday available. This need for artificially generated sources of nuclear particles led to the development of several varieties of particle accelerators.

1.5   Quest for High Energies

The simplest particle accelerators use hundred to thousand kilovolt (kV) static potentials to accelerate charged particles shown in Figure 3. With this design the particle energy is

directly proportional to the voltage across the accelerator. Therefore, to generate high

energy particles a high voltage is required.
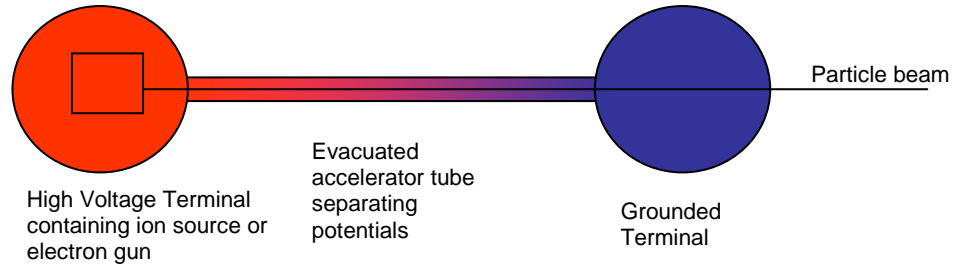
Figure 3. Drawing of basic electrostatic accelerator. Charged particles are emitted at the left and travel to the right. For example, if electrons are being accelerated the high voltage terminal will be negatively charged compared to ground.

Several methods of generating high voltages were attempted, some of which will now be

described.

1.5.1   The Surge Generator

Surge generators consist of capacitors charged in parallel from a DC source and then

discharged through cross connected spark gaps; shown in Figure 4. These high voltage

surges of current have duration of a few milliseconds, and were initially developed for

testing electrical equipment. GE's Pittsfield plant was able to produce surges of over 6

million volts (MV) in 1932 [7]. In 1930 A. Brasch and F Lange applied a 2.4 MV surge

of 1000A through a vacuum chamber of alternating rings of metal and fiber compressed

between end plates [8,9]. The resulting electron beam was allowed to enter the air

through a metal foil window at one end where it produced an intense blue glow extending

one meter. It can be presumed that there were nuclear disintegrations in this region but

they were not identified. However, due to the intensity of the surge the discharge tube

had to be cleaned and reassembled after nearly every surge.
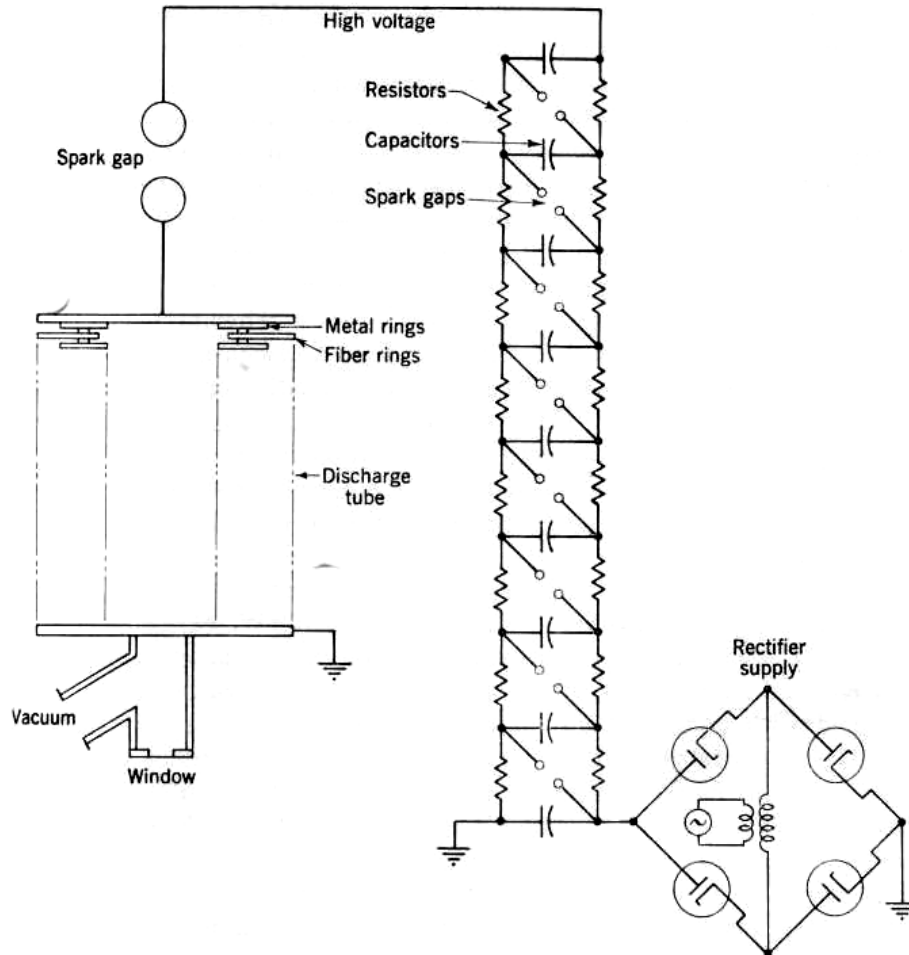
Figure 4. Diagram of Brasch and Lange's surge generator and discharge tube. The high voltage supply circuit is at right and discharge chamber is at left. Taken from Ref. [8].

1.5.2 The Cascade Generator

In the early 1920's an engineering test installation [10] was developed by R.W. Sorenson

for Southern California Edison Company. He utilized three 250 kV transformers in series

powered by 220 kV 50 Hz long distance power lines, shown in Figure 5, to generate peak

voltages over 1MV. In 1928 this system was used by C.C. Lauritsen to generate X-rays up to 750 kV [11] and then in 1934 to generate positive ions of 1 MV [12]. Note that this accelerator's potential oscillated at 50 Hz.
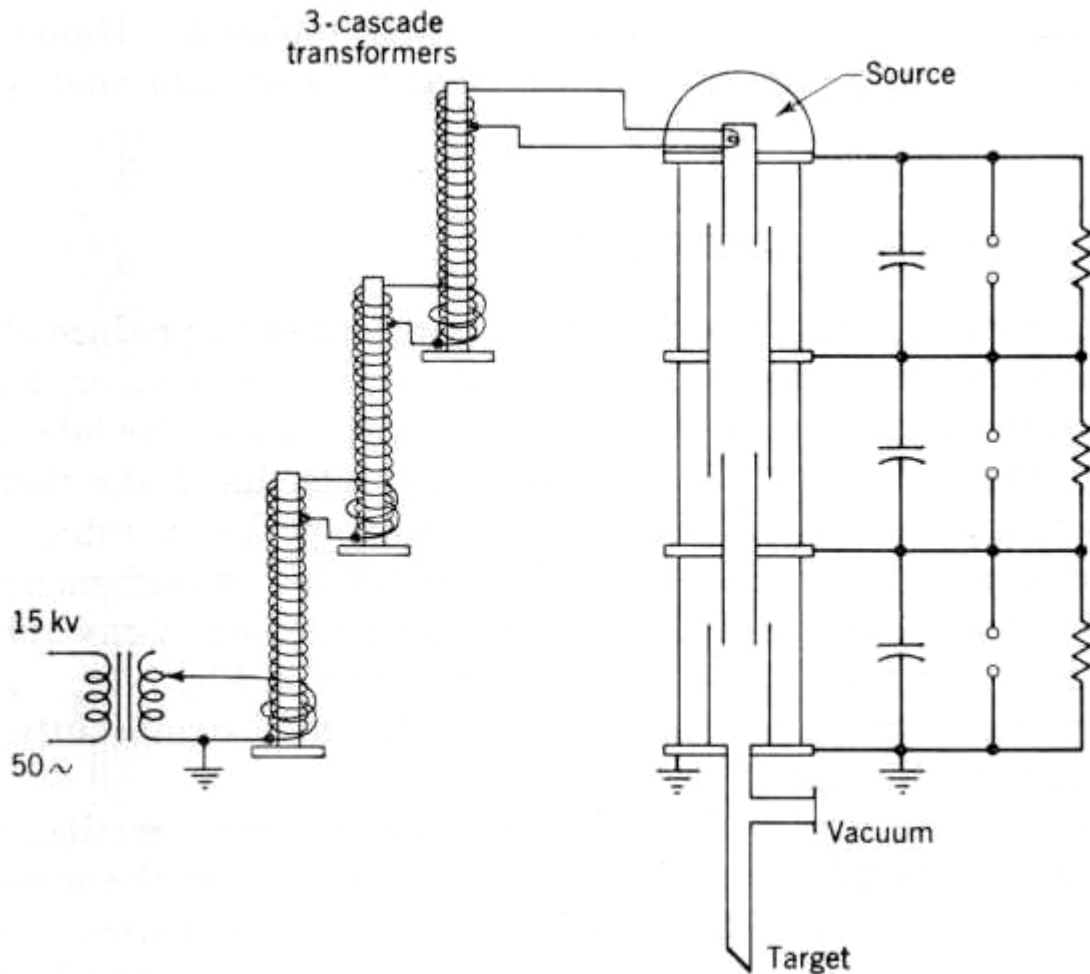
Figure 5. Diagram of the 0.75 MV Cascade transformer and discharge tube at the California Institute of Technology. High voltage supply lines are at left. This voltage is multiplied by three transformers before being put across the discharge tube. Taken from Ref. [10].

1.5.3 The Tesla Coil

As shown in Figure 6, the Tesla coil is a resonance transformer with a high voltage capacitor and spark gap tuned such that both circuits have the same resonance frequency

(typically 25 kHz-2 MHz). Tuve, Breit, Dahl and Hafstad attempted to use a Tesla coil to accelerate a proton beam starting in 1930 [13,14,15,16]. They reported peak potentials of up to 5 MV. However, they found that at 300 kV charge built up on the glass accelerating tube, pierced through it and a sizable current traveled down the tube. They utilized Coolidge tubes which consisted of alternating rings of metal and glass rings to fix this problem. This allowed charge to be more evenly distributed since charge can travel freely through conductors. Due to the rectifying nature of x-ray tubes, these were ideal for use with the AC HV from the Tesla coil. In 1933 D.H. Sloan achieved 1.25 MV x-rays with this method [17].
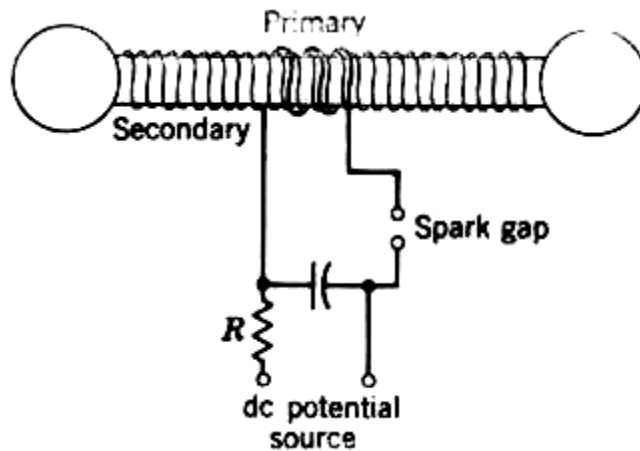
Figure 6. A drawing of a double ended Tesla coil. The primary and secondary coils have the same resonant frequency. Taken from Ref. [18].

1.6 The Cockcroft Walton Generator

Cockcroft and Walton developed a voltage multiplier circuit and used it to break apart lithium nuclei in a target [19,20,21]. This was the first intentional use of a particle accelerator for nuclear disintegration. Originally they planned for 700 kV, but in 1929 Gamow [22] and Condon and Gurney [23], utilizing wave mechanics, showed that

protons of 500 keV had a significant probability of penetrating the potential barriers of light nuclei. Therefore, Cockroft and Walton modified their goal to 500 kV. Their design was an AC circuit utilizing rectifiers to generate a DC potential by charging capacitors in parallel and then discharge them in series through a load resistor, as shown in Figure 7.
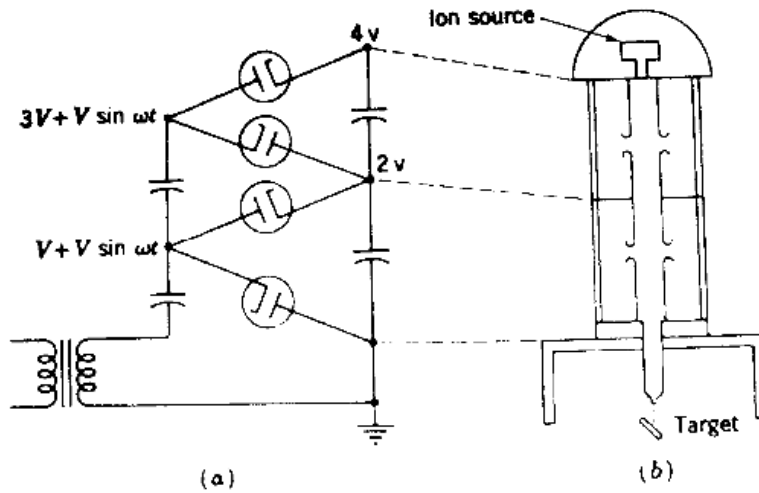
Figure 7. Schematic of a Cockroft Walton generator. The AC voltage is multiplied and rectified by circuit (a) where it is applied to the accelerator at (b) at various electrodes such that a uniform electric field is produced. To generate higher potentials more stages can be added. Taken from Ref. [19].

This is important, as all earlier attempts were either pulsed or AC. A DC high voltage allowed a constant stream of monoenergetic particles to be produced. The accelerator tube was stacked vertically within a glass vacuum chamber embedded with electrodes. An ion source placed at the upper terminal used a high voltage discharge to ionize hydrogen gas. This design reached a maximum potential of 1.25 MV at the Cavendish Laboratory [24], but few designs generated higher than 1 MV. This design is still in use today as a pre-accelerator of particles for injection into higher-energy machines, such as

the Los Alamos Neutron Science Center's 800 MeV Clinton P Anderson linear accelerator.

1.7   The Van de Graaff Accelerator

Robert Van de Graaff described [25] in 1931 a design for a high voltage generator that used silk belts to transfer charge to two 24 inch diameter high voltage terminals, one positive and the other negative. Charge was transferred via corona discharge from needle points located at the base and inside the high voltage terminal onto a rotating insulating belt. The belt carried the charge with it into the high voltage terminal. Once inside the high voltage terminal, another set of needle points allowed the charge to move onto the conducting sphere.   A Van de Graaff generator is shown in Figure 8.
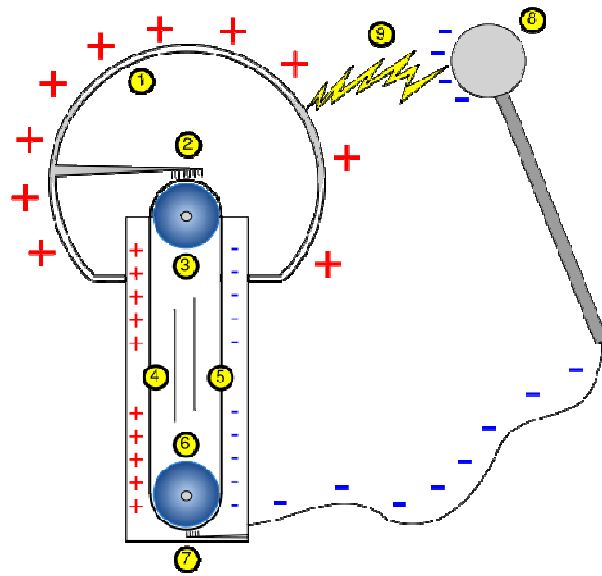
Figure 8. Charge is sprayed onto the belt at needle points (7) via the potential difference created by the triboelectic effect by roller (6) rubbing on the belt. It is brought up to the top needle points (2), where it is forced off by the potential generated by roller (3) rubbing on the belt. In addition negative charge can be brought down the belt if it is sprayed onto the belt.

16

This system attained 1.5 MV. The potential reaches a maximum when the rate current is moving up the belt is equal to the rate at which charge is leaving the high voltage terminal through sparking, corona discharges, etc. Van de Graaff, van Atta, Northrup, and others continued by constructing the Round Hill Electrostatic Generator, shown in Figure 9, capable of producing a potential difference of 5.1 MV [26].

Figure 9. Picture of Round Hill generators. They generated a potential of 5.1 MV. Taken from Ref. [26].

This design consisted of positive and negative 15 ft diameter spheres each charged by two belts, a negative carrying belt and a positive carrying belt. The belts were 4 ft wide and made of insulating paper. Difficulties with humidity led to potential less than the theoretical 10 MV. The positive terminal was charged to 2.4 MV and the negative was charged to 2.7 MV, giving a potential difference of 5.1 MV. In addition, there were difficulties in mounting the accelerating tube leading to a redesign in 1940, giving a working accelerator capable of producing 2.75 MV [27].

Tuve et al. [28] adopted Van de Graaff's design and built a 600 keV accelerator in 1933, only one year after Cockroft and Walton completed their accelerator. This generator accelerated protons using a 1 m diameter spherical high voltage terminal. In 1935 they constructed an accelerator with a 1 m diameter high voltage terminal and a 2 m diameter intermediate voltage dividing shell. This accelerator had a maximum energy of 1.3 MeV for protons.

R.G. Herb [29] was first to use a pressurized insulating gas around the high voltage terminal along with the concentric voltage dividing shields to generate 750 keV protons in 1935. Nitrogen and Carbon dioxide were tested as an insulating gas in addition to air, but air was found to be the most advantageous [30,31]. He followed with designs for 2.4 MeV in 1938 [32] and 4.0 MeV in 1940 [33]. J.G. Trump continued this pressure insulation design, shown in Figure 10, at MIT with Van de Graaff to produce the highest potential ever for a single stage accelerator of 9 MV [34].

In 1947, Herb began to commercially produce accelerators by forming the High Voltage Engineering Corporation, where they developed the first tandem accelerators, shown in figure 11. These accelerate negative hydrogen ions toward a positive high voltage terminal, strip them of their electrons via a hydrogen gas jet, and then accelerate the protons back down to ground potential, thereby using the potential difference twice.
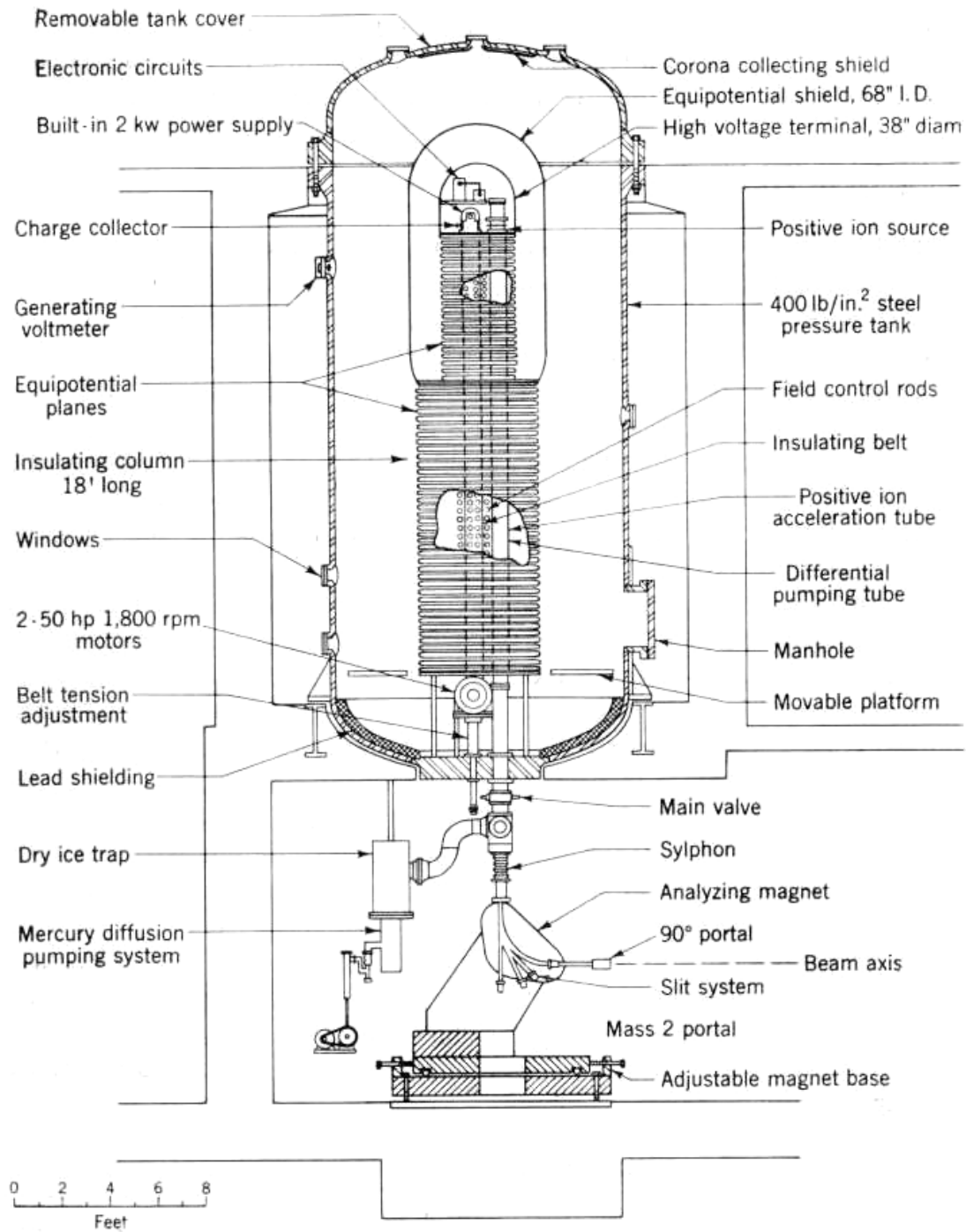
Figure 10. MIT's 9 MV electrostatic accelerator. The accelerator was built into a pressurized chamber to minimize voltage losses. Taken from Ref. [13].
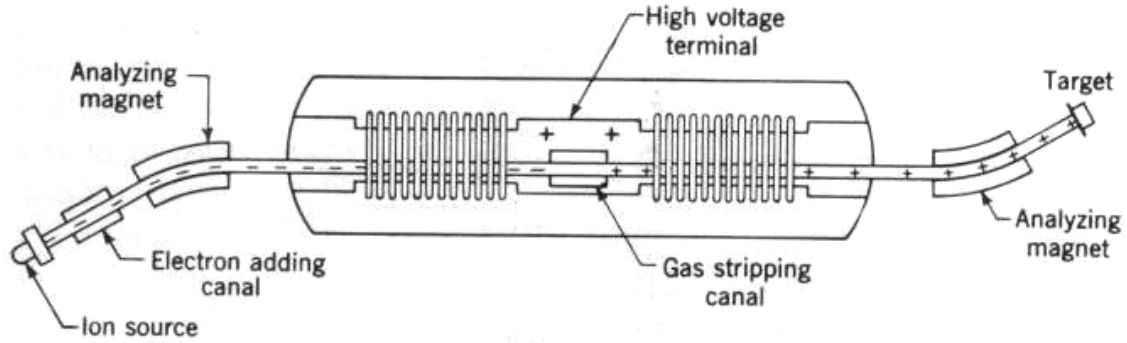
Figure 11. Drawing of a two-stage tandem electrostatic accelerator. Negative ions are fed into the accelerator at left. Nonnegative ions are removed by the first analyzing magnet. The negative ions are then accelerated through the first potential. Then they are stripped of their electrons by passing through a jet of hydrogen gas. These positive ions are then accelerated again. The last analyzing magnet strips the beam of any non-positive ions. Taken from Ref. [35].

1.8   Cyclotrons and Other Modern Accelerators

Lawrence and Livingston's 1.2 MeV proton cyclotron [36] of 1929 introduced a new way of accelerating particles which did not need such extreme voltages to obtain high energies. The cyclotron uses a magnetic field to bend a particle's trajectories into a spiral path such that it is accelerated multiple times by the same electrodes. Similarly, modern cyclic synchrotrons and linear accelerators utilize multiple smaller "kicks" as opposed to just one large potential difference like electrostatic accelerators. These accelerators apply varying electric and magnetic fields to beam pulse packets, which are timed to always be accelerating the pulse. The pulses are shielded from the electric field as it is altered. The maximum center of mass energy of particle accelerators is plotted as a function of this in Fig. 12 known as a Livingston Plot. Two of the most energetic accelerators in the world currently are synchrotrons, the Tevatron at Fermilab (1 TeV) and the LHC at CERN (7 TeV).

However, electrostatic accelerators are still used to introduce particles into larger accelerators, and can be used whenever lower energies and excellent voltage regulation are needed, such as medical facilities, due to their low cost and ease of operation.
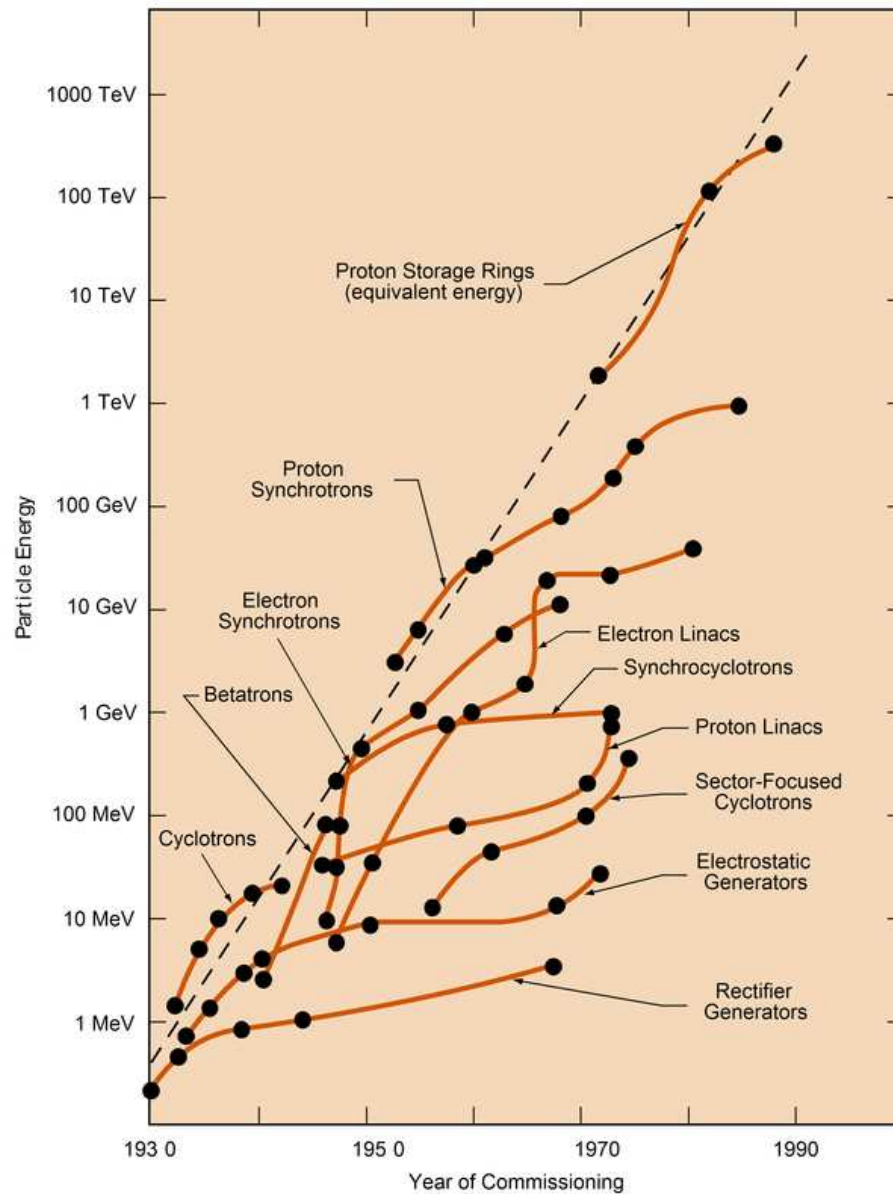
Figure 12. Livingston Plot of accelerator energy versus year of commissioning. More modern designs greatly eclipse the maximum energy of the largest electrostatic generators. Taken from Ref. [37].

1.9   Amateur Electrostatic Accelerators

While most attention in physics research has been devoted to the highest energy accelerators, there is still interesting science to be done with low energy accelerators, even by amateurs. The original idea for the small accelerator described in this paper was generated by an article by F.B. Lee in 1959 [38]. Lee built an electrostatic accelerator with a three foot long Pyrex accelerating tube and copper rings to ensure a uniform electric field, shown in Figure 13. It was powered by a Van de Graaff generator. Vacuum pumps were built from refrigerator compressors to reduce cost.
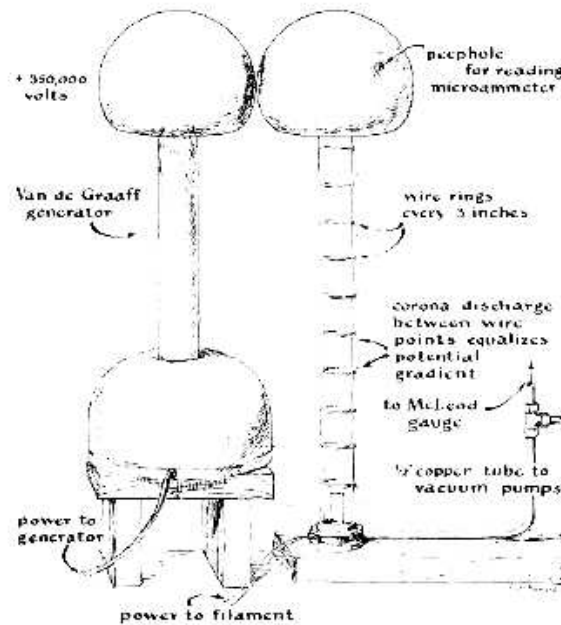
**Figure 13. Drawing of Lee's electrostatic accelerator. The filament
is mounted at the bottom of the accelerating tube with the target
inside the high voltage terminal. Taken from Ref [39].**

A similar accelerator was built by Larry Cress in 1971 [39] to accelerate deuterium. In 1992 Fred Niell, a high school student at the time, constructed a 20 stage Cockroft Walton voltage multiplier which generated 100 kV used to power a simple electrostatic accelerator[40].

22

Chapter 2

THEORY OF ELECTROSTATIC ACCELERATOR OPERATION

In this chapter the general theory of operation of the Van de Graaff generator, accelerating column, and the electron gun will be discussed.

2.1 Generation of the High Voltage Accelerating Potential

The electric field that accelerates electrons down the accelerating tube is formed by the potential difference between the high voltage terminal and ground. In a Van de Graaff accelerator, shown in Figure 14, the high voltage is produced by a Van de Graaff generator. Van de Graaff generators use an insulating belt that brings charge from the base to the conductive high voltage terminal, which is separated from the base by an insulating column. A motor drives the belt via pulleys (see Fig. 8). In small Van de Graaff generators, the difference in the electronegativity of the belt and the pulleys, as they rub against each other, produces a potential difference. In our Van de Graaff generator the pulley gains a positive charge. In larger Van de Graaff generators high voltage power supplies are used to spray charge without the need to use the triboelectric effect. Directly next to the pulley/belt interface is a grounded wire brush. Electrons are drawn from the brush toward the pulley, but are intercepted and deposited in the belt.

Once the electrons are on the belt they can not move along the belt because it is an insulator. Inside the high voltage terminal a similar pulley/wire brush is installed with the exception that the electronegativity is reversed and the drawn to the outside of the conductor. Once on the high voltage terminal, the charge equalizes its distribution since the high voltage terminal is a sphere. In our accelerator the high voltage terminal is

23

rounded into the shape of a capsule in order to minimize sharp points where charge will build up, and to allow space for electronics to be mounted inside. Any sharp point on the high voltage terminal will result in charge build up and a much larger electric field near the point, possibly reaching the ionization potential of air and sooner causing a corona discharge. The condition for corona discharge between two wires can be calculated using Peeks's law [41]

$$e = mg\delta r \ln\left(\frac{S}{r}\right) \tag{1}$$

where e is the corona inception voltage, m is the irregularity of the wires (1 for polished wires), r is the radius of the wires, S is the separation of the wires in meters, g is the visual critical potential gradient given by

$$g = g_0\delta\left(1+\frac{0.301}{\sqrt{\delta r}}\right) \tag{2}$$

where g_0 is the disruptive critical potential gradient (for air equal to approximately 30 kV/cm), δ is the air density factor given by

$$\delta = \frac{3.92P}{T} \tag{3}$$

where P is the pressure in torr, T is the temperature in Kelvin. This formula can be modified by adding the appropriate geometrical correction terms to suit different setups.
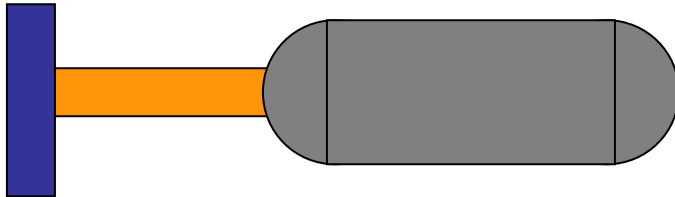
Figure 14. Diagram of high voltage terminal and Van de Graaff generator. Charge moves from ground at the blue base, up the orange column via belts, and is put onto the conducting capsule. The conducting capsule is electrically insulated from ground.

The high voltage terminal can be treated as a spherical capacitor which has capacitance

$$C = 4\pi\varepsilon_0 r \qquad (4)$$

where r is the effective radius of the high voltage terminal, and ε_0 is the permittivity of free space. The capacitance forms from the separation of charge being held on the high voltage terminal that is electrically isolated from ground. From this the voltage V on the sphere can be calculated using

$$Q = CV \qquad (5)$$

where Q is the charge on the sphere. Taking the time derivative of Eq. 5 results in

$$\frac{dQ}{dt} = i = C\frac{dV}{dt} \qquad (6)$$

where i is the current entering or leaving the spherical high voltage terminal. The terminal is charged by the Van de Graaff generator, which gives a constant current into the high voltage terminal for a given belt speed, and is discharged by any current leaving the sphere, either current moving down the accelerating tube, in the form of column current or beam current, or corona discharge into the air. From Eq. 6 it can be seen that the voltage will peak when the current is zero, or when the up-current from the Van de Graaff generator is equal to the current leaving the high voltage terminal. The current leaving can be approximated with an Ohm's law like term describing the corona discharge and column current, and a constant beam current term

$$i_d = \frac{V}{R} + i_b \qquad (7)$$

where R is the effective resistance. This approximation is only valid when corona discharge is small however since the corona discharge current is not linear with respect to

voltage in air. Therefore, the potential on the high voltage terminal is the solution to the differential equation

$$C\frac{dV}{dt} = i_u - \frac{V}{R} - i_b \tag{8}$$

where i_u is the current supplied by the Van de Graaff generator and i_b is the beam current, both constants. Eq. 8 has the solution

$$V = (i_u - i_b)R\left(1 - e^{\frac{-t}{RC}}\right) \tag{9}$$

if $V=0$ at time $t=0$. As time progresses the voltage will move toward

$$V = (i_u - i_b)R \tag{10}$$

Therefore, to obtain maximum potential a large up-current is needed along with good insulation from ground and small beam current. Since the resistance between any two concentric rings is approximately the same, and the current going through all of the rings is the same, the potential drop between any two adjacent rings will be the same. The electric field is given by

$$\vec{E} = -\vec{\nabla}V \tag{11}$$

From this we can see that since the potential is changing at a constant rate along the axis of the accelerating tube, the electric field will be uniform and directed straight down the tube. This ensures that accelerated electrons will continue focused to the target.

If the high voltage terminal is simplified to a sphere the maximum voltage in air can be more easily obtained. The electric field outside a uniformly charged sphere is

$$\vec{E} = \frac{Q}{4\pi\varepsilon_0 r^2}\hat{r} \tag{12}$$

where Q is the charge on the sphere, and r is the distance from the center of the sphere. This can be reduced by using Eqs. 4 and 5 to

$$rE = V \qquad (13)$$

where r is the radius of the high voltage terminal and E is the electric field produced at r. The maximum E field possible in air is determined by the onset of dielectric breakdown which occurs at approximately 3,000,000 *V/m*. Using the 12.5 cm radius of the high voltage terminal for the sphere generates a maximum possible voltage of 375,000 V. Therefore, to obtain a higher voltage than this on the high voltage terminal either the radius of the high voltage terminal, or the dielectric strength of the medium needs to be increased. For example, pressurized sulfur hexafluoride is commonly used in the electrical industry for circuit breakers, switchgear and other high voltage equipment since it has one of the highest dielectric breakdown values. With a 375,000 V potential the maximum energy of an electron is given by

$$T = qV = 375{,}000 \ eV \ . \qquad (14)$$

Another concern is the possibility of discharges between the rings. Besides producing a very uniform electric field, this is one reason so many rings are needed. Measurements were made with two 20.32 cm side square sheets of aluminum separated by a sheet of high density polyethylene of thickness 1.27 cm. The maximum high voltage prior to sparking was approximately 7000 V. If one assumes a linear relationship to separation, then the maximum voltage will be 3400 V since the accelerator rings are 0.62 cm thick. With 48 rings this allows a maximum potential of 160,000 V. However, with this design the number of rings can be increased if needed, since the accelerating tube can be

disassembled. In the future more rings could be added assuming that the nylon rods can withstand the additional tension. In the end, there are multiple possible factors which limit the maximum possible potential.

2.2   The Electron Gun

The electron gun provides the electrons that are accelerated down the potential gradient in the acceleration column. The current electron gun is taken from a RCA 3RP1 cathode ray tube [42], which had been cut in half across the symmetric axis, shown in Figs. 15-17.
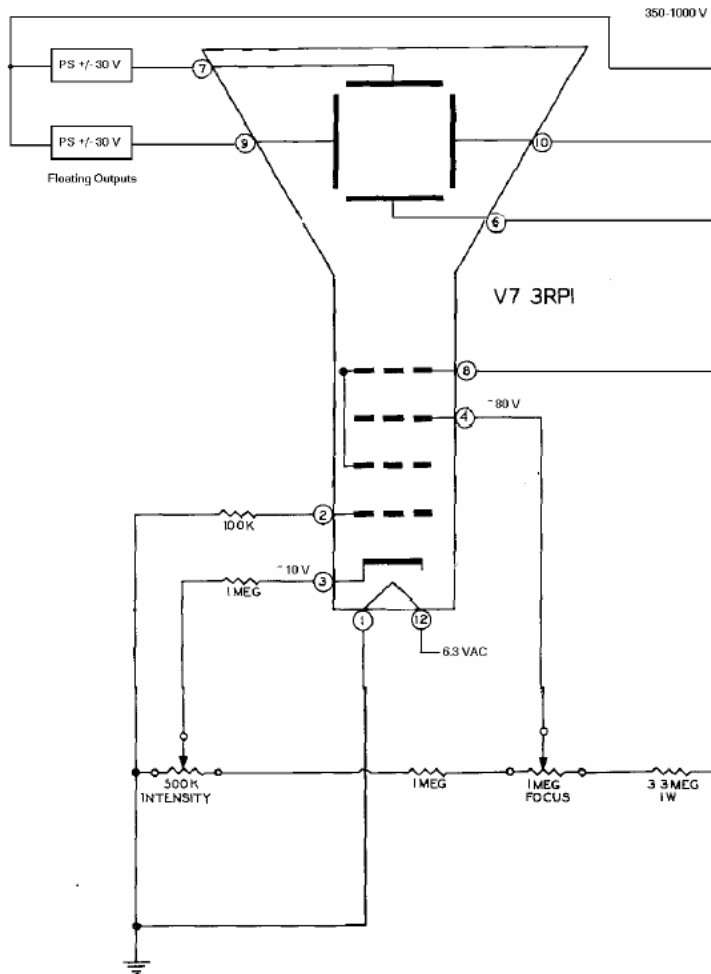
Figure 15. Biasing schematic for RCA 3RP1 cathode ray tube. The cathode (pin 3) is heated by the filament (1, 12). Once heated the cathode will begin to emit electrons. The intensity grid (2) limits electrons without sufficient energy from passing by. The focus grid (4) changes the focal point of the beam. The accelerating grid (8) determines the energy of the electrons upon leaving the gun. Grids 9,10 and 6,7 deflect the beam on the two axis perpendicular to the beam axis.

Deflection Grids   Accelerating Grid   Focusing   Filament   Connection to
                                                Grids   /Cathode   electronics
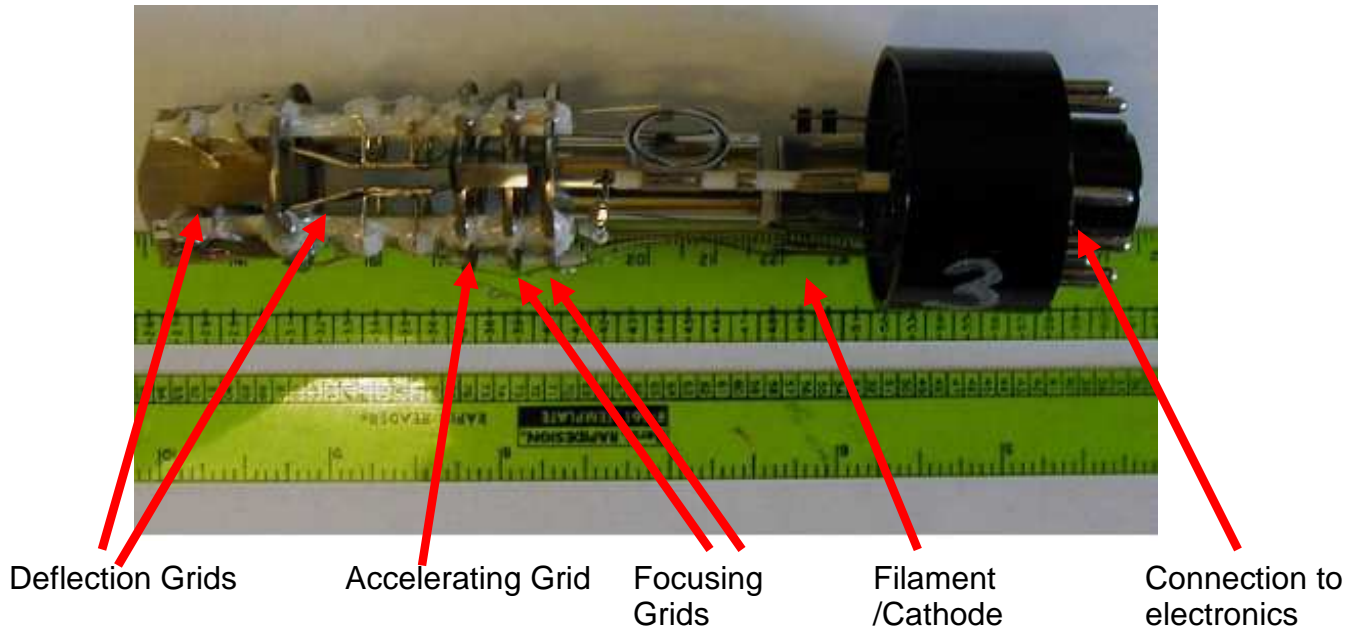
Figure 16-Picture of electron gun of RCA 3RP1 CRT. The glass casing has been removed.
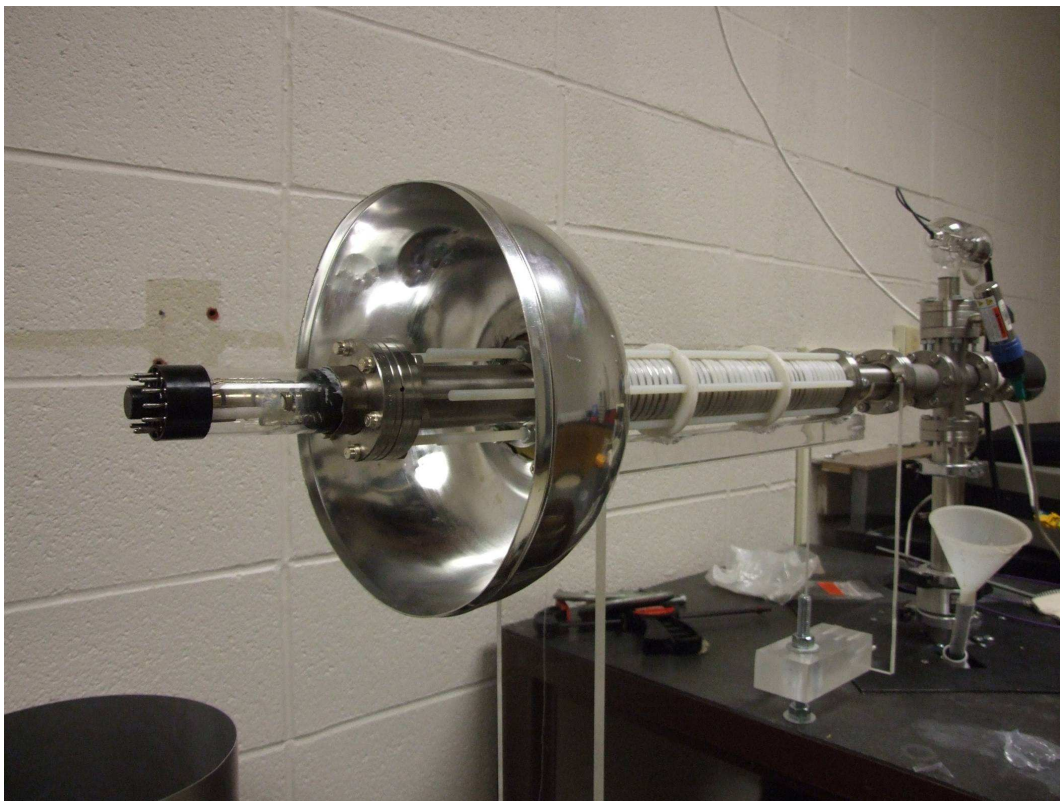
Figure 17-Picture of electron gun inside the high voltage terminal. The Van de Graaff generator and high voltage terminal shell have been removed.

The electron gun functions by resistance heating of a filament by a current of 0.6 A. Tungsten filaments operate at temperatures of 2000-3300 K depending on filament shape, size, and quantity of current. The filament heats the cathode, which has a low work function such that it will eject electrons through thermionic emission when heated. The cathode is coated with a metallic oxide. Early hot cathodes used barium oxide. Modern designs use combinations of barium, strontium, aluminum, calcium or thorium oxides [43]. The filament heats the cathode to typical operating temperatures of 1100-1300 K. The cathode is kept at the full potential of the accelerator.

The electrons emitted from the cathode have energies of a few eV. The current emitted is given by the Richardson-Dushman law:

$$J = \frac{4\pi m k^2 e}{h^3} T^2 e^{\frac{-W}{kT}} \tag{15}$$

where J is the current density (amps/m^2), k is Boltzmann's constant (8.62 x 10^{-5} eV/K), h is Planck's constant (4.135 x 10^{-15} eVs), m is the mass of the electron, e is the charge and W is the work function of the cathode. Typical work functions are a few eV. The electrons will have a distribution following the Maxwell-Boltzmann distribution. Assuming that the electrons are non-relativistic such that

$$p^2 = 2mE \tag{16}$$

the probability density of emitting an electron with energy between E and $E+ dE$ is given by:

$$f_E dE = f_p \left(\frac{dp}{dE} \right) dE = 2\sqrt{\frac{E}{\pi (kT)^3}} e^{-E/kT} dE \tag{17}$$

which is equivalent to a chi squared distribution (see Figure 18) with three degrees of freedom

$$f_E \, dE = \chi(x,3) \, dx \quad \ni x = \frac{2E}{kT} \tag{18}$$

$P_r(x)$
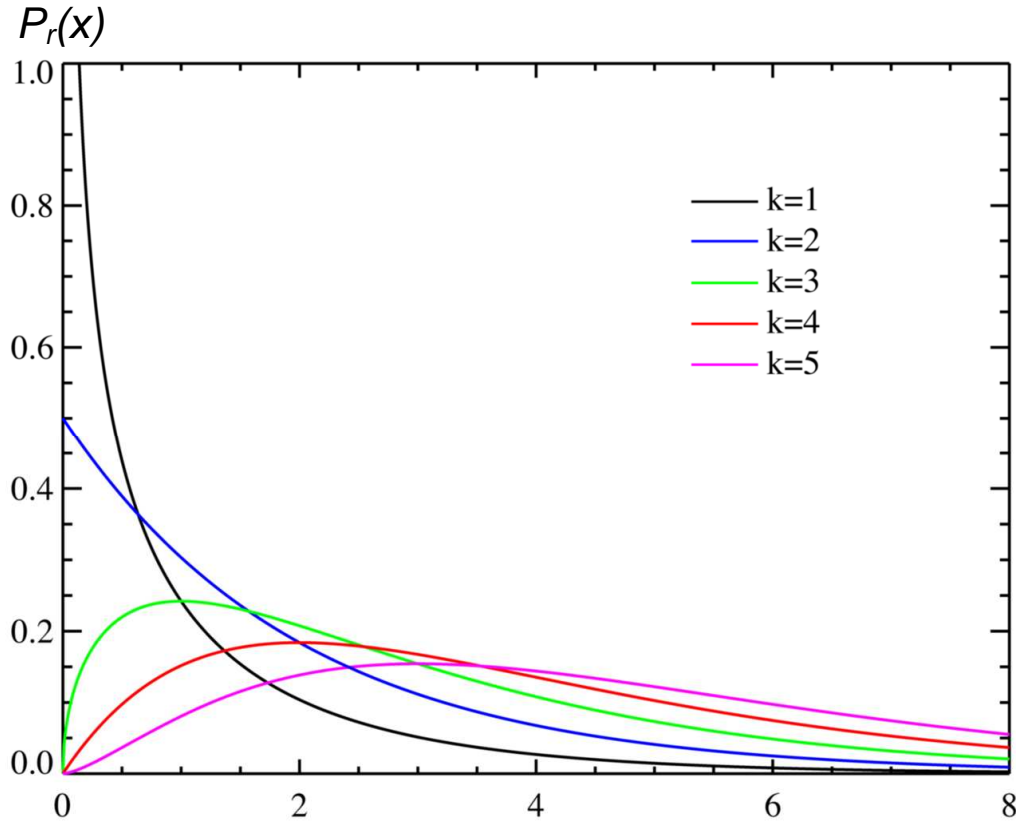
Figure 18-Plot of Chi-squared distribution probability density functions. k denotes the degree of freedom. For the Maxwell-Boltzmann distributions that electrons off the cathode follow k=3 (green line)

Electrons leave the cathode in all directions but are focused by other components of the electron gun.

Downstream of the cathode is the control grid. Under typical operation the control grid is at the same potential as the cathode, allowing all electrons to pass through. However, if less beam current is desired, then the potential of the control grid can be changed to a few

volts below the cathode voltage. This will allow only the electrons that have enough energy to pass over the potential barrier to pass through the control grid, and will reduce the electrons according to the Maxwell Boltzmann Distribution.

After this the electrons move toward the focusing grids which generate an electric field that focuses the electron beam. Multiple electrodes are used to construct an Einzel lens shown in Figure 19. The field created by the electrodes bends the electrons outwards and then inwards to a focal point. The focal length can be to be adjusted to match the effective length of the accelerator.
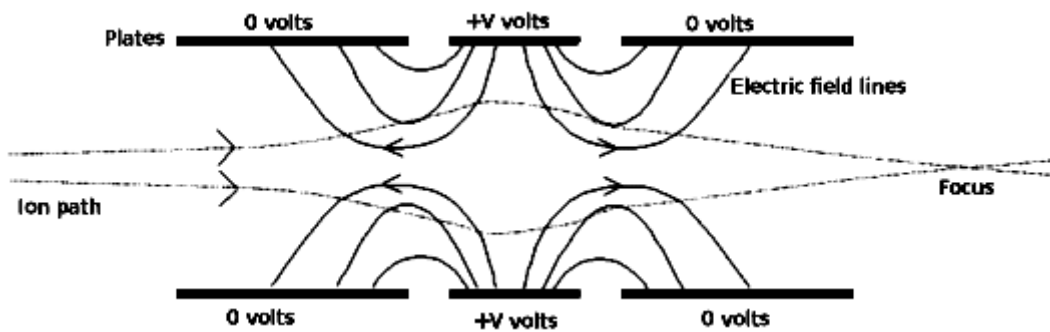
Figure 19. Diagram of Einzel lens. Incoming unfocused electrons are bent outwards and then inwards to a focal point.

After this the electrons move past the accelerating grid where they receive a larger boost in energy. The accelerating grid typically operates at 500-2000 V below the potential of the cathode.

Before entering the accelerating tube the electrons can also be bent in either off axis direction by two sets of deflection plates, one for each axis. A potential difference is placed between the two plates of a set which will bend the electron beam in the direction

of lower potential. Due to the uniform electric field in the accelerating tube, electrons should continue to be focused toward the target.

At the other end of the accelerator is a phosphorescent screen. When electrons strike a conductive fluorescent material which the screen is coated with a green glow is emitted. An insulating ceramic tube can be placed between ground and the screen such that a microammeter can be utilized to measure the beam current. However, using a phosphorescent screen as opposed to a Faraday cup could lead to the phenomenon of secondary emission where additional electrons are released when the electrons from the particle beam strike the screen. This could cause the measurement of the beam current to be too low.

Chapter 3

HISTORY OF THE HOUGHTON COLLEGE ELECTROSTATIC ACCELERATOR

3.1   History of Houghton College Electrostatic Electron Accelerator

For the purpose of performing low energy nuclear physics experiments a small electrostatic accelerator is being built at Houghton College. Several iterations of the accelerator design have been produced prior to the current design. However, these accelerators have shared some common design features. To produce high voltages a Van de Graaff generator is used. Inside the high voltage terminal, an electron gun utilizing a hot cathode emits electrons to be accelerated down an accelerating tube to ground. The accelerating tube is fitted with equipotential conducting rings centered along its axis. These act as a voltage divider through the action of the corona discharge current down the accelerating tube. By equally spacing the conducting rings a uniform potential gradient is created. This ensures a uniform electric field down the accelerating tube, accelerating the electrons down the axis of the tube. The system is kept evacuated by a diffusion pump backed by a rotary forepump and liquid nitrogen cold trap.

3.1.1   Original Design (2002)

In 2002 the first electrostatic accelerator was completed [44] shown in Figs 20-21. It featured a glass accelerating tube 110.7 cm in length and 3.8 cm in diameter with copper wire wound into equipotential rings on the outside of the tube.

A homemade electron gun, shown in Fig. 22, was constructed with a filament, cathode and accelerating grid taken from a cathode ray tube. The cathode, was at a potential of 100V which was powered by batteries.
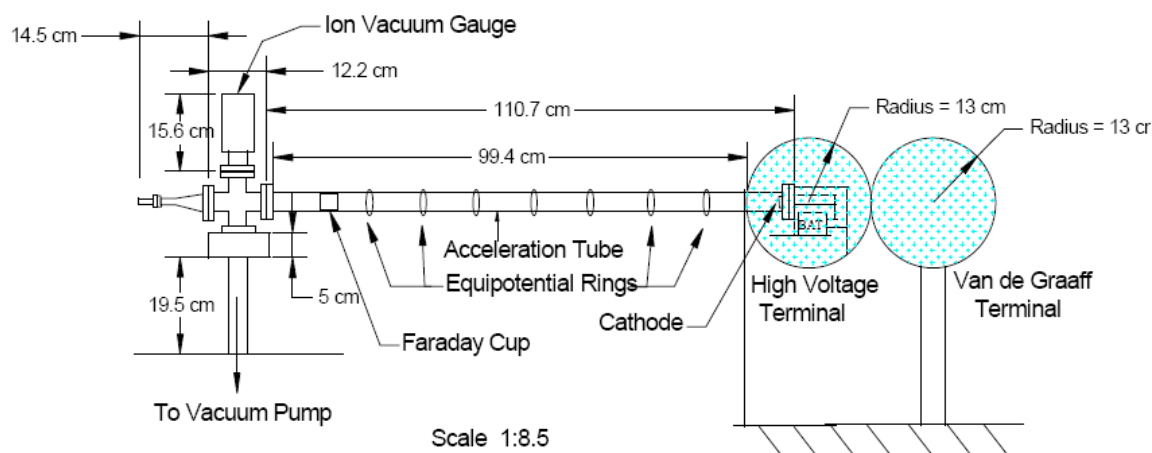
Figure 20. Scale drawing of original design. Electrons were accelerated from the electron gun at right to the Faraday cup at left where the beam current was measured. Equipotential rings were added to ensure a uniform electric field. Taken from Ref. [44].
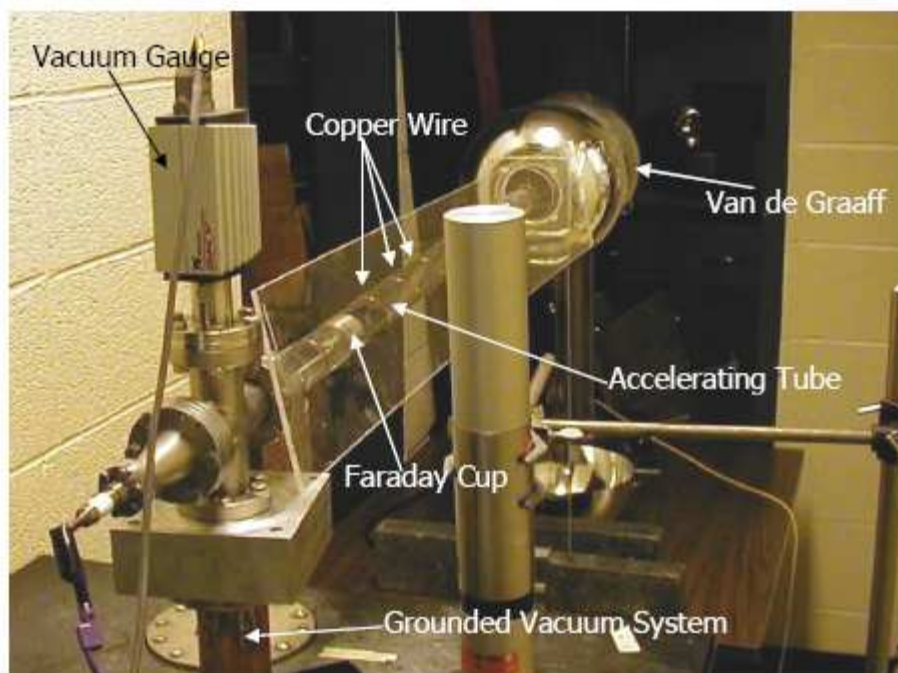
Figure 21. Picture of original design. The Van de Graaff generator is at the rear. The vertical cylinder near the front is a plastic scintillator that was used to measure the energy spectrum of the Bremstrahlung X-rays. Taken from Ref. [45].

35
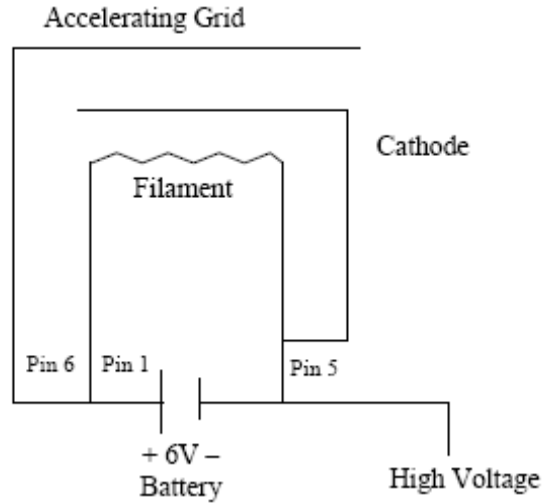
Figure 22. Schematic of electron gun. Only the filament voltage and the accelerating voltage are able to be controlled. Taken from Ref. [44].

This design produced beam currents of up to 4 μA into a faraday cup. Shown in Fig. 23

is the beam spot.

Figure 23. Photograph of beam spot on phosphorescent screen. Note the relatively unfocused beam spot.

This design had some major flaws however. Charge built up on the walls of the glass

tube, causing the beam to be deflected after a short time. In addition, high voltage

discharges occurred near where the tube entered the HV terminal, ionizing residual gas in

the accelerating tube and producing bursts of current even when the filament of the

electron gun was cold.

3.1.2   Epoxied Insulating and Conducting Rings (2004)

In order to correct the issues of the previous design a new accelerating tube was constructed and tested in 2004 [45], shown in Fig. 24. This tube consisted of alternating of 51 0.3 cm thick 10.16 cm diameter 5052 aluminum rings and 51 0.6 cm thick 9.14 cm diameter high density polyethylene rings. They were aligned with 1/4" delrin rods and sealed with Hysol Epoxi-Patch EPK 1C vacuum epoxy. The rings were fabricated using a Sherline Products model 5400-CNC computer controlled milling machine.

Figure 24. Photograph of accelerator tube. The electron gun mounts to the left. The brass flange on the left is machined to mate with the high voltage terminal.

The electron gun was modified by attaching a 1.3 cm diameter 7.4 cm long copper tube to form a new accelerating grid, shown in Fig. 25-26. A 0.32 cm hole was drilled in the front cap. The copper tube was mounted 0.2 cm in front of the control grid, which was what used to be the accelerating grid in the previous design. The accelerating grid was powered by eleven 9V batteries in series. The filament was powered by 5 1.5V C cell batteries in series.
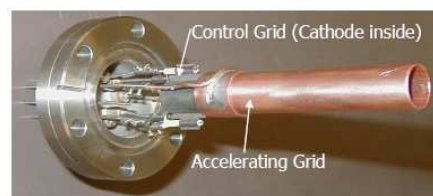
Figure 25. Photograph of electron gun with copper tube accelerating grid mounted. The rest of the electron gun was taken from a RCA 3RP1 cathode ray tube. The long copper tube was attached to ensure that the electrons would enter the accelerating tube where the field was uniform. Taken from Ref. [45].
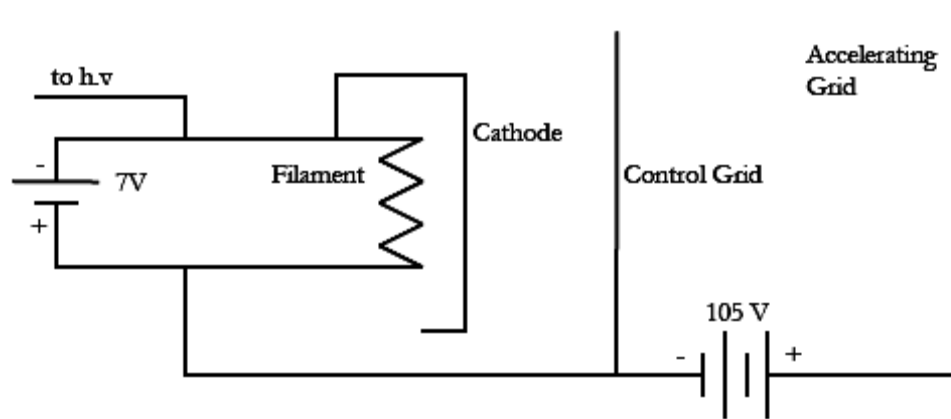
Figure 26. Circuit diagram of electron gun. The addition of a control grid allowed the intensity of the beam current to be controlled by removing electrons below an energy threshold according to the Maxwell-Boltzmann energy distribution. Taken from Ref. [45].

Figure 27. Photograph of accelerator. Electrons are accelerated from left to right down the accelerating tube. The Van de Graaff generator is used to generate the high voltage.   The faraday cup measures the beam current. Taken from Ref. [45].

This design, shown in Figure 27, corrected the problems of the previous design and

produced up to 0.4 μA of current, which went away when the filament was turned off,

unlike previous designs.   However, as shown in Figure 28, the beam spot was not

uniform.   The endpoint to the bremsstrahlung radiation curve was about 180 keV

measured by a plastic scintillator shown in Figure 29.
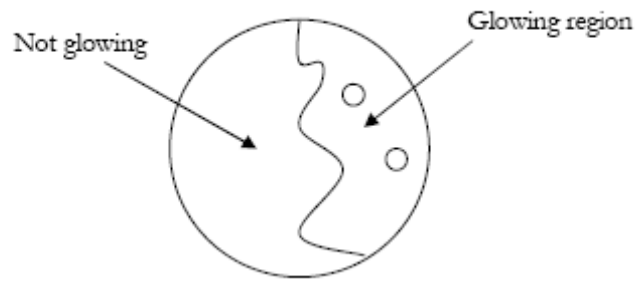
Figure 28. **Drawing of approximate shape of beam spot. Note that the beam is very unfocused and irregular. Taken from Ref. [45].**
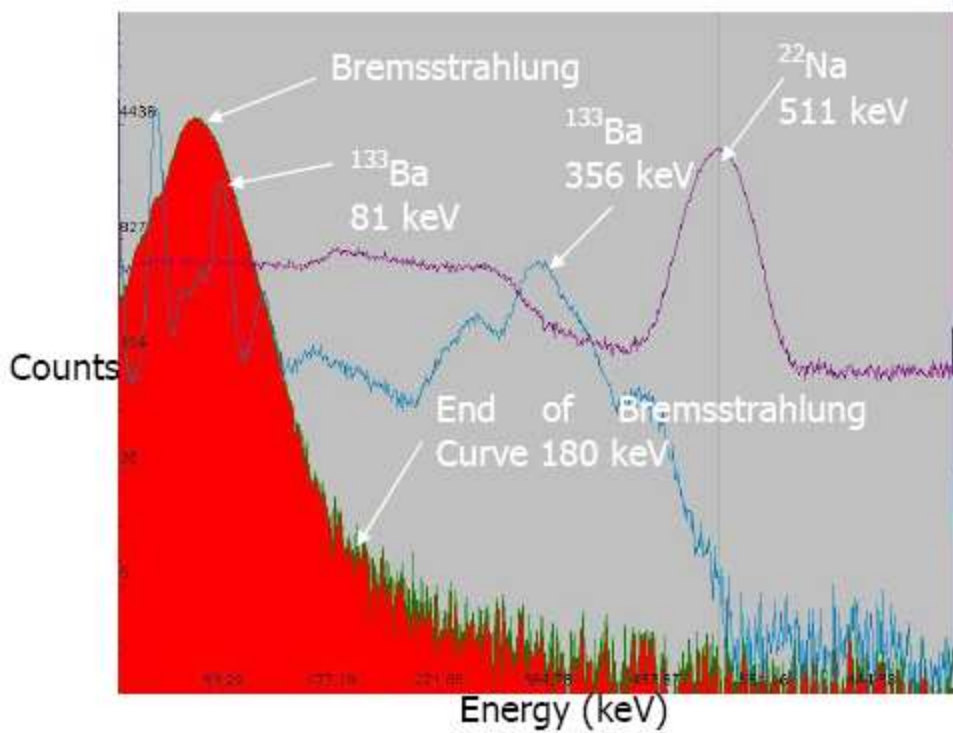
Figure 29. **Plot of counts versus energy of Bremsstrahlung x-ray radiation. The end point is at approximately 180 keV. Ba-133 and Na-22 were used to calibrate the energy scale. Taken from Ref. [45].**

However, soon after these initial measurements the accelerating tube began to leak. An attempt was made to locate the leaks by spraying the rings one at a time with isopropyl alcohol and waiting to observe if a pressure fluctuation occurred. The accelerating tube was then patched with additional vacuum epoxy. However, despite multiple attempts, the

39

tube continued to leak and could not achieve the necessary 10^{-5} torr vacuum. Also, there were concerns that multiple layers of vacuum epoxy would lead to inconsistency in the resistance between the rings, hence a non-uniform electric field.

In addition, the electron gun could not be focused in order to correct the large beam spot and there was no way to control the state of the electron gun once the high voltage terminal was assembled. In order to change the voltages of the electron gun the high voltage terminal had to be taken apart. Tuning of the electron gun voltages could only be done by changing the number of batteries used.

3.1.3 Compressed Viton O-Rings (2006)

In 2006 several new accelerator tubes were designed and tested relying on compressed Viton o-rings. The first design used 50 5.08 cm outer diameter, 1.36 cm inner diameter, 0.152 cm thick stainless steel washers interspaced with 3.81 cm outer diameter, 1.905 cm inner diameter, 0.236 cm thick Teflon washers with the Viton o-rings exterior to the Teflon washers, since Teflon is permeable to air shown in Fig. 30. Teflon was chosen as it acts as a good electrical insulator, so that the voltage divider principle can still be used.

Figure 30. Drawing of ring stacking. Teflon rings (black) were sealed by Viton O-rings (red) and compressed between stainless steel washers (orange). Taken from Ref. [46].

This lead to an uncompressed 19.4 cm long accelerating tube. The design was tested with steel threaded rods to compress the array of rings onto vacuum flanges but the system pressure could not be reduced to less than a 10^{-2} torr vacuum. The difficulty centering the washers and o-rings lead to uneven compression of the o-rings, causing leaks. Another attempt with larger S.A.E. Standard stainless steel washers also suffered sealing problems due to the rough mating surface.

3.1.4   Current Design

The current design utilizes 48 high density polyethylene 0.62 cm thick rings with viton o-rings compressed into interior glands with 5.08 cm outer diameter, 1.27 cm inner diameter 0.15 cm thick stainless steel washers (see Figure 31-33). All but two of the plastic rings have a 5.08 cm outer diameter and 1.91 cm inner diameter. The other two plastic rings are larger with 6 holes for the ¼ inch nylon threaded rod to pass through which compresses the rings. The o-rings are 3.33 cm outer diameter, 3.31 cm inner diameter, 0.16 cm thick. They fit into glands in the polyethylene rings that are 2 mm thick with inner diameter of 1.37 cm, outer diameter of 1.93 cm.

Figure 31. 3D rendering of rings. The standard polyethylene ring is at the left, the polyethylene ring with threaded rod guides is at center, and the stainless steel washer is at left. Taken from Ref. [46].

Figure 32. Photograph of assembled accelerating tube. The high voltage terminal mates to the large brass disc at left.
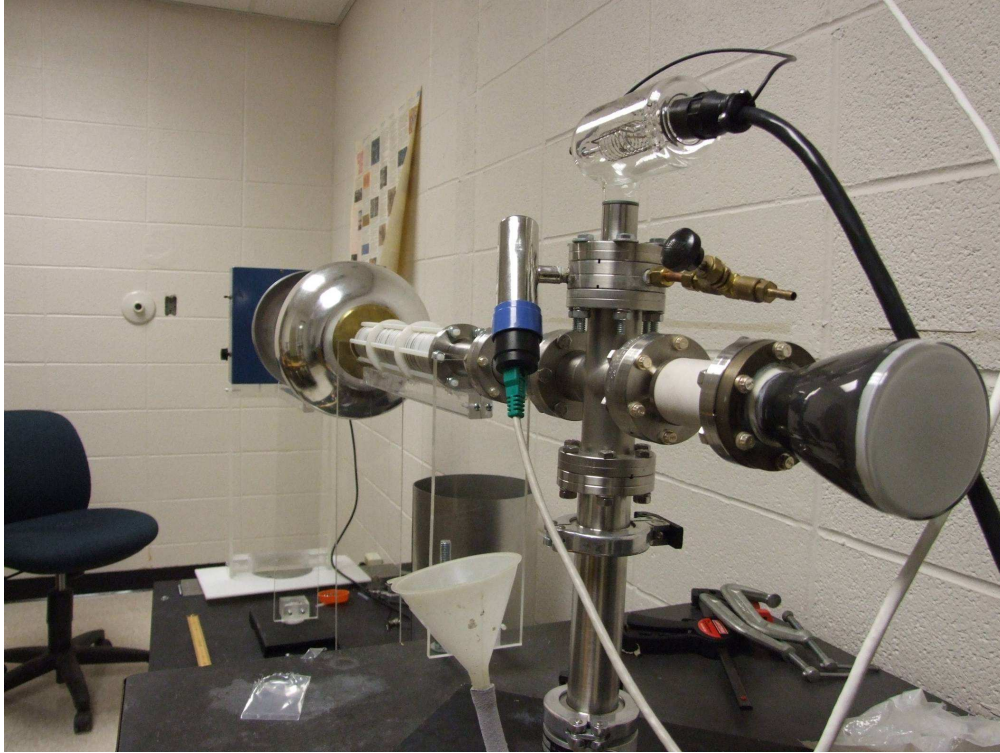
Figure 33. Photograph of the current experimental setup. Electrons will be accelerated from the high voltage terminal at the rear to the phosphorescent screen at the front. The vacuum system is mounted below. The accelerating tube is mounted on an acrylic support base.

The initial tube was tested with ¼ inch nylon threaded rod and could achieve 10^{-5} torr vacuum. However, over a period of days it was discovered that the nylon rods would stretch and the system could no longer achieve this vacuum. To remedy this, acrylic threaded rods were constructed for their high tensile strength and resistance to stretching. However, these rods were extremely brittle, prone to breaking, and difficult to thread. When under the required stress they would eventually shatter. Finally, the original ¼

inch nylon rods were pre-stretched by 2-3 cm prior to installation on the accelerating tube. This design was able to provide adequate tension that allowing a pressure 10^{-5} torr to be maintained.

In addition, a new electron gun was constructed to be used with new control electronics. The previous designs had poorly focused beam spots due to an overly simple electron gun design that lacked a focusing grid. Also, the electron gun could not be controlled remotely; the high voltage terminal had to be opened to turn the gun on or off. A new electron gun was constructed by cutting an RCA 3RP1 cathode ray tube in half, removing the phosphorescent screen, and utilizing the filament, cathode, focusing and accelerating grids. The Faraday cup of the previous design was replaced with the phosphorescent screen of the 3RP1 which was grounded by attaching a wire from the conducting film on the screen to the flange on which the screen was epoxyed. An insulating ceramic tube was mounted between the phosphorescent screen and the grounded chamber (see Fig. 34) allowing a microammeter to measure beam current.

Figure 34. Picture of phosphorescent screen. The white ceramic tube electrically isolates the screen from the grounded vacuum system at left.

This design was tested at low accelerating voltage without attaching the Van de Graaff generator or accelerating tube and produced a well defined beam spot of less than one millimeter diameter at a current of 0.2 μA. However, the beam could not be centered electronically and the gun became damaged when mechanical alignment was attempted. Another 3RP1 was cut in half, this time the deflection plates were not removed. This produced a slightly less well defined beam spot of approximately 2 mm with a current of about 0.15 nA shown in Figure 35.
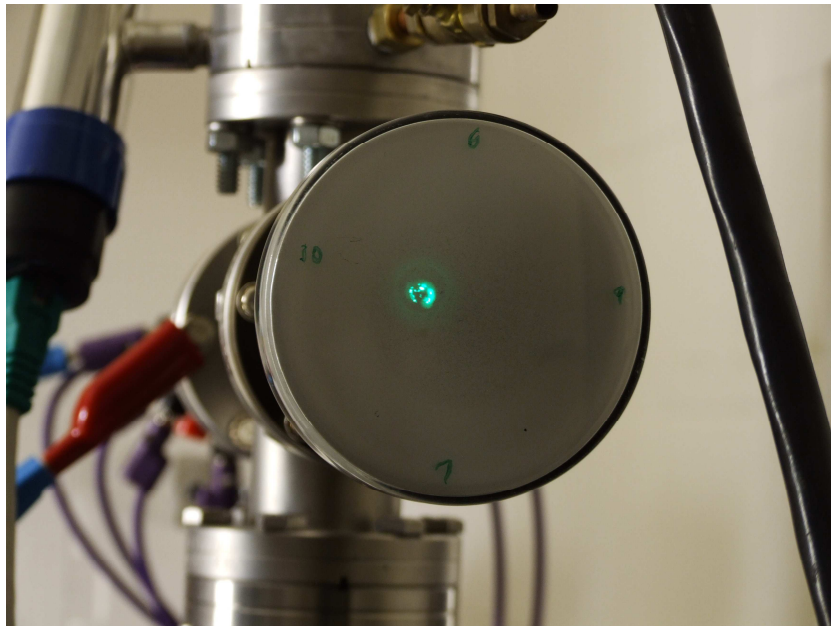
Figure 35. Photograph of beam spot from second electron gun with deflection plates intact. The beam spot is larger and less well defined than the beam spot produced by the first electron gun.

Chapter 4

ELECTRON GUN CONTROL CIRCUIT DESCRIPTION

4.1   Overview

In order to manipulate the voltages on the electron gun electrodes from within the high

voltage terminal a microcontroller circuit was constructed. Due to the large difference in

potential between the microcontroller located in the high voltage terminal and ground,

standard communication cable such as CAT5 Ethernet, GPIB, or RS 232 could not be

used. To solve this problem a nonconductive fiber optic link was used between the

microcontroller in the high voltage terminal and a PC compatible control computer. To

do this, the light pulses from the fiber optic line must be converted to RS 232 needed by

the microcontroller (see Fig. 36).
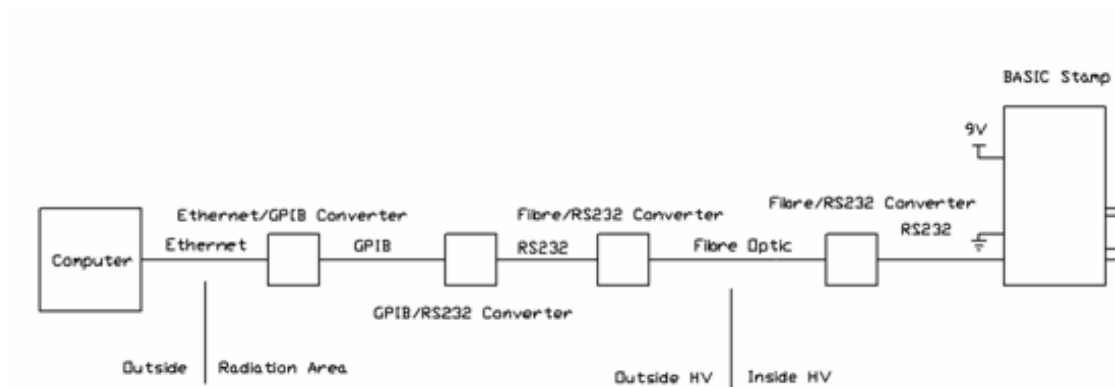
Figure 36.   Block drawing of terminal interface.   A remote computer running LABVIEW communicates via the LAN to a GPIB converter which then goes to a RS232 converter. A fiber optic line takes the signal into the high voltage terminal. The signal is finally converted back to RS232 before being fed into the microcontroller.

After the CTC FIB-232 fiber optic modem is a BASIC Stamp 2 microcontroller that reads

the signal from the modem and outputs binary bits corresponding to the different voltages

of the electron gun. These twelve binary bits are transmitted to a DAC7624 Digital to

Analog converter which outputs four low voltage/low current analog signals shown in

Figure 24. These signals are amplified by four transistor amplifier circuits driving

EMCO G20 DC to High Voltage DC converters which raise the voltages to around 1000

volts. At this point the voltages were placed on the electron gun. The computer will run

LabVIEW and will communicate with the circuit via Houghton's Local Area Network

Ethernet network to a GPIB controller. This controller will then communicate with the

RS 232 converter that leads to the fiber optic cable. The GPIB bus can be used to

communicate with other devices such as pressure gauges and microammeters.
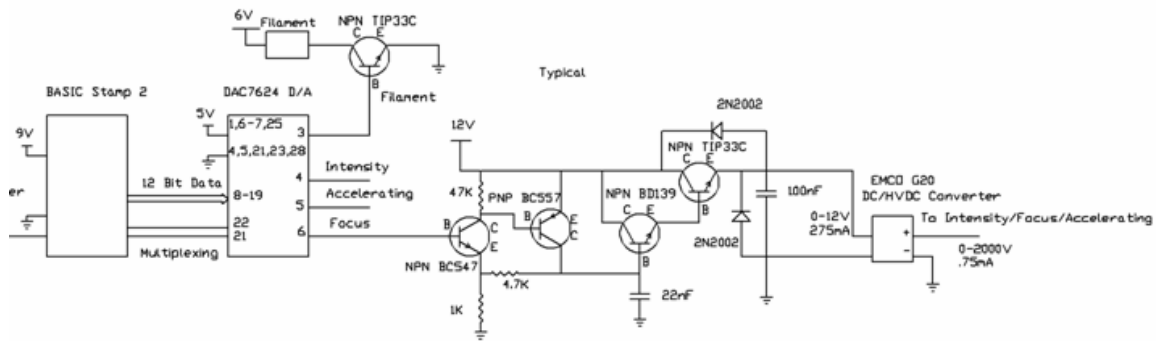
Figure 37. Schematic of control circuit. The microcontroller communicates with a DAC. This DAC controls four separate transistor circuits (one shown): one for intensity, focus, accelerating, and horizontal grids in addition to controlling the filament. After the transistor circuit the signal is fed into DC/HVDC converters before being sent to the electron gun.

4.2 Fiber Optic Modem

Windows HyperTerminal was used to test the controller via the COM1 port Serial/RS-

232 9 pin interface. Eventually an Ethernet to National Instruments eNet controller

GPIB bus will be inserted and controlled with LabVIEW software. A 9-25 pin converter

is used to connect the CTC FIB-232 fiber optic modem (see Figure 38). The computer side modem is powered via the RS-232 line and hence does not require external power. The modem converts the electrical signal from the RS-232 line to two L-Com E12-85T FT4 62.5/125 fiber optic lines, TX and RX (transmit and receive). These lines transmit light pulses through a glass fiber surrounded by layers of cladding and shielding insulation. The two fiber optic lines pass into the high voltage terminal through a hole at the bottom. The modem inside the high voltage terminal is powered by 9V from the microcontroller board's battery because the microcontroller's RS-232 signals are non-standard. The RS-232 data then passes through a null modem which switches the TX and RX lines. Before attaching to the microcontroller the signal passes through a 25-9 pin RS-232 converter.
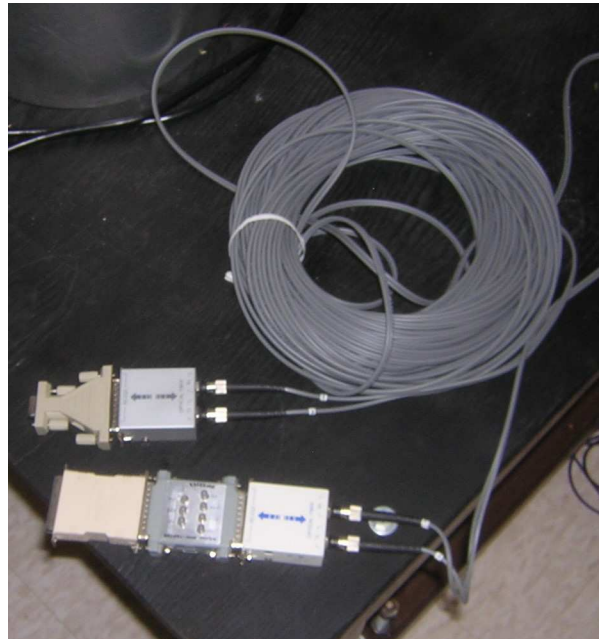
Figure 38. Photograph of fiber optic modems and cable. The modems use two separate TX and RX lines. Appropriate converters are mounted on the ends of the modems.

4.3   Microcontroller

A microcontroller is a computer on a chip. The primary component of a microcontroller is its processor. However, unlike a traditional microprocessor, a microcontroller chip also contains RAM and ROM in addition to other components such that it can operate self sufficiently without requiring other support chips. While not as powerful as a standard microprocessor, a microcontroller can provide rudimentary computing power for a wide array of tasks where a standard computer would be too powerful, large, expensive, or power consuming.

The microcontroller used in this circuit is a Parallax BASIC Stamp 2 [47] mounted on a Parallax Super Carrier Board (see Fig. 39). The Super Carrier Board provides RS-232 serial communication, voltage regulation, input/output ports, and a small prototyping area.
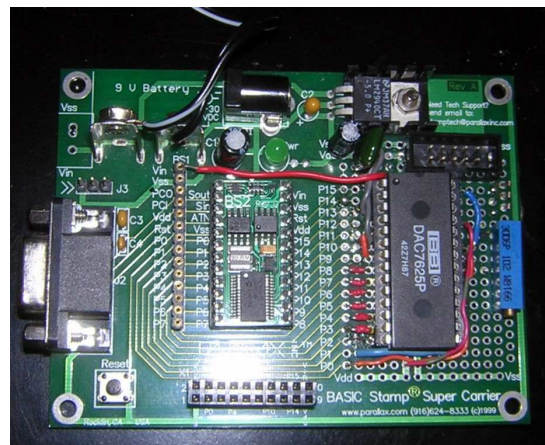
Figure 39.   Picture of BASIC Stamp Super Carrier board.   The BASIC stamp is mounted in the center.   A 9V battery can be attached at the top left but a voltage regulator is also mounted. The serial port is on the left edge. The green board on the right section of the board is used for mounting the DAC. A ribbon cable header at top left connects to the transistor amplifier board.

The BASIC Stamp 2 circuit board itself is a 24 pin DIP with dedicated 20 MHz processor capable of performing 4000 instructions per second, 32 bytes RAM memory, 2K memory EEPROM, and an interface with 16 I/O ports [47]. The circuit board is sized at 1.2"x0.6"x0.4" and draws 3 mA when active. The board is powered by a 9V battery although the regulator will run on 6-30 VDC.

The microcontroller can be programmed with a language known as PBASIC, which is a slimmed down version of BASIC with only 42 commands. The programs written for the microcontroller are stored in the chip's EEPROM. The microcontroller is attached to a computer running Parallax's Windows Editor 2.4 via RS-232 allowing programs to be burned into the EEPROM. The high voltage controller program (Appendix B) asks the user which electrode of the electron gun to modify the voltage, and then which value they wish to assign to that part of the electron gun. This information is put on the output bus to the DAC 7624 Digital to Analog Converter which has 12 bit resolution with 2 multiplexing bits. This allows for 4096 values for the voltage to range.

4.4   Digital to Analog Converter

A Digital to Analog converter is a component which changes a digital value to an analog voltage. The digital signal is composed of binary bits. A binary number is a base two number, which can be represented as a series of zeros and ones, or bits, such that each successive bit is a higher power of two. Each bit is either an on or off state of the circuit. By interpreting all of the powers of two any number can be represented. This digital

signal can be converted back to its analog equivalent. The resolution is determined by the number of analog states and therefore the possible number of digital states. Each successive analog state will be separated by the same voltage since the digital states are separated by the value of the least significant bit (LSB). Many DACs convert the digital signals to analog signals via a resistor ladder; example shown in Fig. 40. A resistor ladder uses chains of resistors that the digital signal's powers are inputted at decreasingly large resistance. Each next less significant bit's output goes through a higher resistance and hence contributes less to the final voltage.
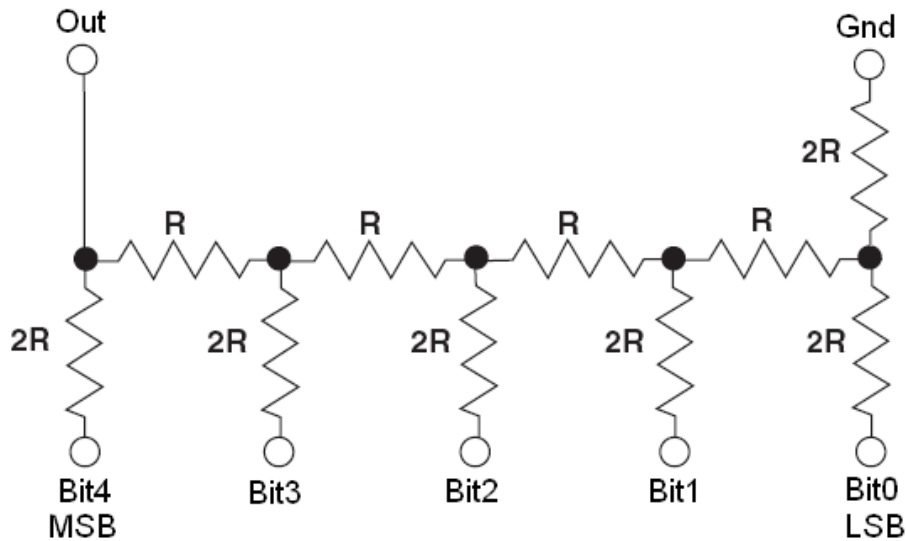
Figure 40. Diagram of 5 bit R2R ladder. The MSB's voltage is applied at the left and goes through the least resistance. The LSB goes through the most resistance meaning that its state contributes the least to the final voltage.

From Ohm's law and Kirchoff's rules the output voltage is given by

$$V_{out} = \frac{V_{\mathrm{Re}f}}{2}\left(D_0 + \frac{D_1}{2} + \frac{D_2}{2^2} + \frac{D_3}{2^3} + \ldots + \frac{D_n}{2^n}\right) \quad (19)$$

Where V_{Ref} is the voltage supplied by the digital source (5 V for TTL), n is the resolution of the digital source, and D_n is the state of the nth digital bit (0 for off, 1 for on). The DAC used in this application is a Burr-Brown DAC7624 12 bit quad voltage output

digital to analog converter [48], outputting 4 separate analog signals. However, to conserve data ports multiplexing functionality is built into the chip. Along with the 12 data bits transferred to the DAC are two multiplexing bits allowing for 4 channels (see Figure 43). Each channel is only modified when the state of the multiplexing bits correlates with the logic truth table shown in Figure 41.

A1	A0	R/$\overline{\text{W}}$	$\overline{\text{CS}}$	$\overline{\text{RESET}}$	$\overline{\text{LDAC}}$	SELECTED INPUT REGISTER	STATE OF SELECTED INPUT REGISTER	STATE OF ALL DAC REGISTERS
L[1]	L	L	L	H[2]	L	A	Transparent	Transparent
L	H	L	L	H	L	B	Transparent	Transparent
H	L	L	L	H	L	C	Transparent	Transparent
H	H	L	L	H	L	D	Transparent	Transparent
L	L	L	L	H	H	A	Transparent	Latched
L	H	L	L	H	H	B	Transparent	Latched
H	L	L	L	H	H	C	Transparent	Latched
H	H	L	L	H	H	D	Transparent	Latched
L	L	H	L	H	H	A	Readback	Latched
L	H	H	L	H	H	B	Readback	Latched
H	L	H	L	H	H	C	Readback	Latched
H	H	H	L	H	H	D	Readback	Latched
X[3]	X	X	H	H	L	NONE	(All Latched)	Transparent
X	X	X	H	H	H	NONE	(All Latched)	Latched
X	X	X	X	L	X	ALL	Reset[4]	Reset[4]

Figure 41. DAC logic truth table. A0 and A1 are the multiplexing bits. R/W, CS, and LDAC, are set to ground. Reset is set to 5V. Taken from Ref. [48]

To maintain the state of channels not currently selected registers are used to store the data. Due to the small number of bits needed, the registers are constructed of flip flop logic memory. Each channel has its own R-2R ladder shown in Fig 42. However, the maximum current output of the R-2R ladder is small so operational amplifiers are used on each channel to boost the current.
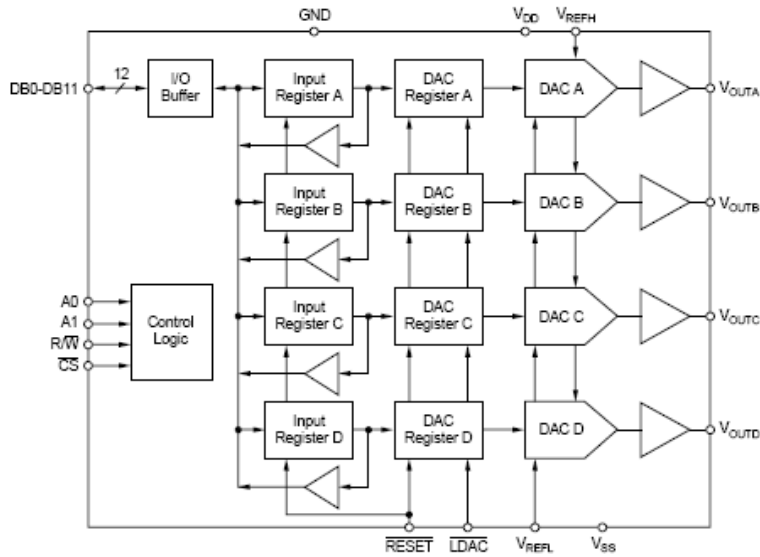
Figure 42. Block diagram of DAC. Note that all data comes from the same I/O buffer, but each channel has its own dedicated registers, R-2R ladder, and Op Amp. Taken from Ref. [48]
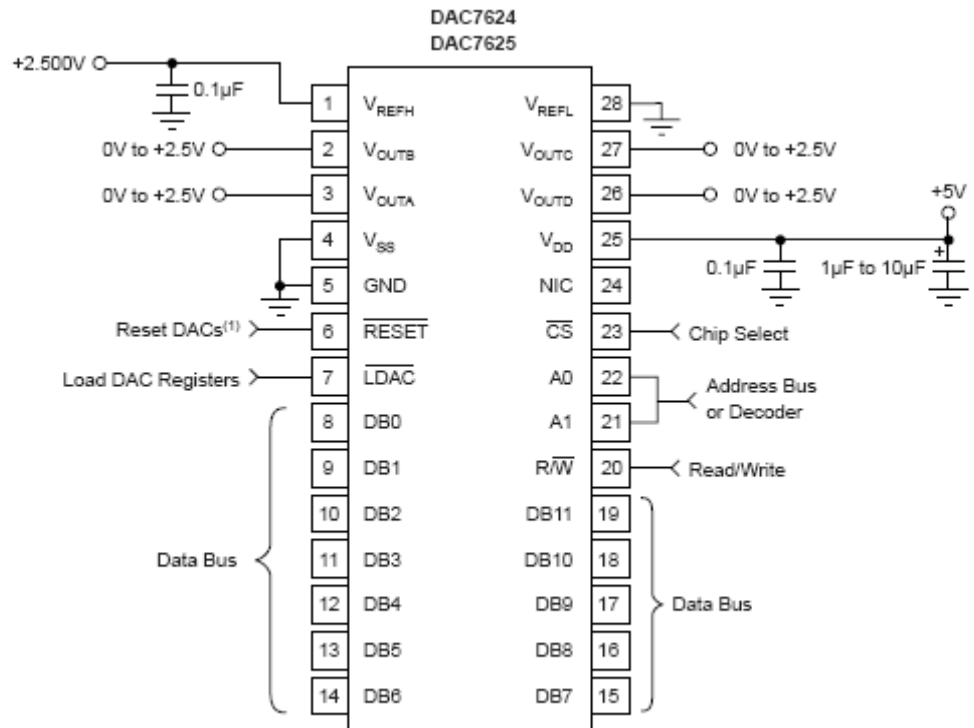

Figure 43. Pinout of DAC7624 with typical usage. A0 and A1 are used for multiplexing, DB0-DB11 are the digital inputs, VoutA-D are the analog outputs. Taken from Ref. [48].

For consistent output levels well regulated reference voltages are required. The DAC requires a 5V supply voltage as well as a 2.5V reference. The 5V voltage supply is taken from the microcontroller's voltage regulator. Initially the 2.5V reference was taken from a voltage divider circuit. However, as the value of the DAC's output changed the current drawn by the DAC changed. This would cause the voltage supplied by the voltage divider circuit to change, and thus made the DAC behave in a non-linear way. To rectify this situation an additional voltage regulator was installed. A LM317 voltage regulator was chosen because the output voltage can be set with a potentiometer. The R/W, CS, and LDAC pins are grounded and the reset pin is set to 5V according to the logic truth table. Each channel outputs 0-2.5V with up to 1.25 mA of current. Since the DAC is 12 bit there are 2^{12}=4096 different output values. This gives a resolution of 0.610 mV. The four outputs are sent to separate amplifiers for the intensity, focus, accelerating, and vertical grids. The DAC chip is mounted into a DIP socket that is soldered on the prototype area of the BASIC Stamp Super Carrier Board. The outputs are sent via a 10 wire ribbon cable header to another circuit board where the transistor amplifiers are mounted.

4.5   Transistor Amplifier Circuit

Due to the fact that the DAC can only output 1.25 mA of current a transistor based amplifier is used to increase current capacity. The high voltage converter chips require up to 275 mA at full load. A transistor amplifier circuit shown in Fig. 44-45 was designed from a similar one designed by Guido Socher [49] for use in a DC power supply.
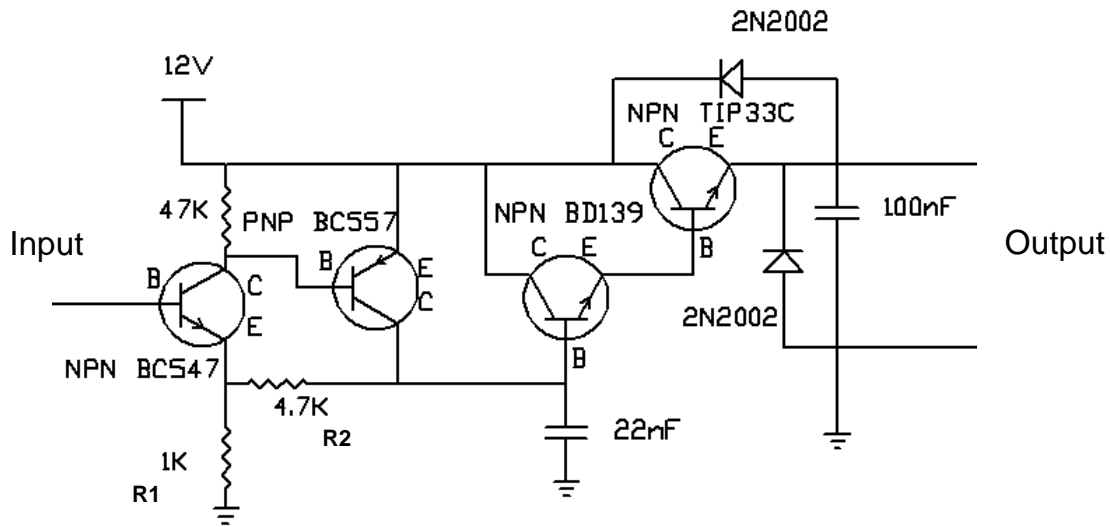
Figure 44-Schematic of Transistor amplifier circuit. Input comes from DAC, and the output goes to EMCO G20 HVDC converter.

The transistor circuit multiplies the voltage by a factor of 5.7 since

$$Amplification = \frac{R1 + R2}{R1} = \frac{4.7 + 1}{1} = 5.7 \qquad (20)$$

A transistor circuit was used rather than an operational amplifier (op amp) circuit because op amp circuits need to be buffered from highly capacitive loads such as the high voltage converters. An op amp was initially tried but led to a high frequency oscillation in the output of the high voltage converters. This was eliminated by the addition of a 5 μH inductor and a 27 Ω resistor in parallel with the output of the op amp, but this came at the cost of increased resistive losses which increased power demands. In addition, the use of this transistor amplifier eliminates the need for a negative supply voltage that the op amp needed, which complicated the power supply needed to power the circuit.

The transistor circuit can be divided into two sections. The side with the BC547 and BC557 acts as a voltage amplifier. The side with the TIP33C and the BD139 power transistor acts as a current amplifier in the configuration known as a "Darlington transistor" [49]. The output of the circuit is limited by the TIP33C power amplifier which can supply approximately 70 W of power at maximum. This equates to 5.8 A at 12 V, well beyond the needs of the high voltage converter circuit. Of note is that each transistor is initially in the "off" state. Therefore, no oscillations should occur upon applying power since none of the circuit's amplifier's outputs are being activated. The outputs are stabilized from small fluctuations via the use of diodes and capacitors.
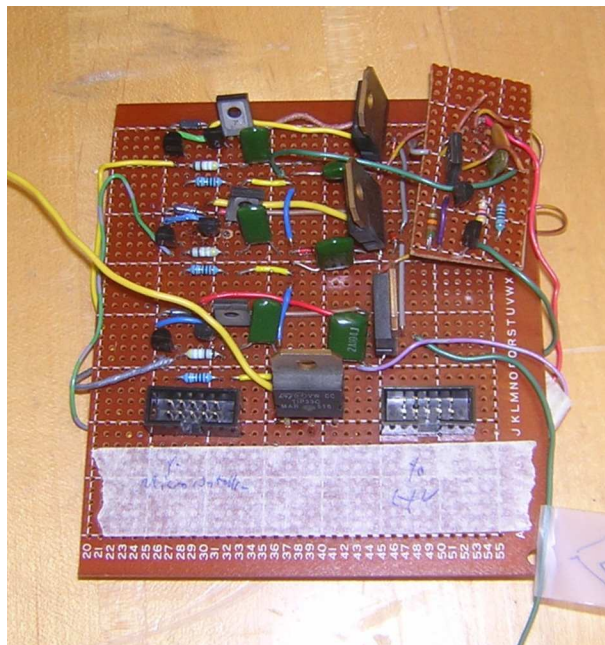
Figure 45. **Photograph of transistor amplifier board. Four separate transistor amplifiers are mounted on this board. Signal comes from the microcontroller/DAC board and output to the HVDC converter via ribbon cables.**

Each of the four DAC outputs has its own dedicated transistor amplifier. The outputs are led to a plexiglas board with the HV converters via a ribbon cable. The circuit is

powered by 8 D cell batteries connected in series to supply the required 12V. This 12V could also be supplied to the microcontroller, as the super carrier board has its own voltage regulator on board. The power transistors are mounted with heatsinks.

4.6   High Voltage Converter

In order to boost the voltage from 12 volts to the ~1000 volts required by the electron gun four EMCO G20 HVDC Converters are used. Each HVDC converter is mounted in a black epoxy shell and measures 1.5x1.5x0.63 inches as shown in Figure 46.
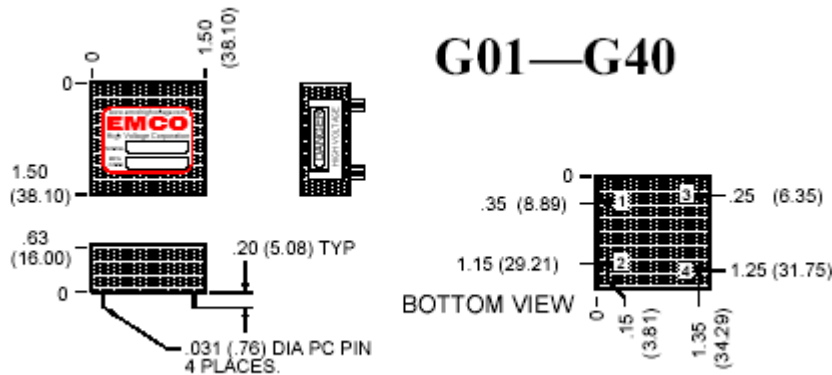
Figure 46. Physical dimensions of HVDC converter. Pin 1 is the positive input, pin 2 is the negative input, pin 3 is the positive output, and pin 4 is the negative output. Taken from Ref. [50]

The converters have two input pins and two output pins. The input pins take the supplied voltage from the transistor amplifier of 0-12V using less than 100 mA with no load, and less than 275 mA at full load supplying the maximum of 0.75 mA output current. Upon reaching the turn on voltage of ~0.7V the HVDC converter linearly multiplies the input voltage to obtain an output voltage range of 0-2000V (see Figure 47) with maximum current of 0.75 mA.

TYPICAL INPUT vs. OUTPUT VOLTAGES
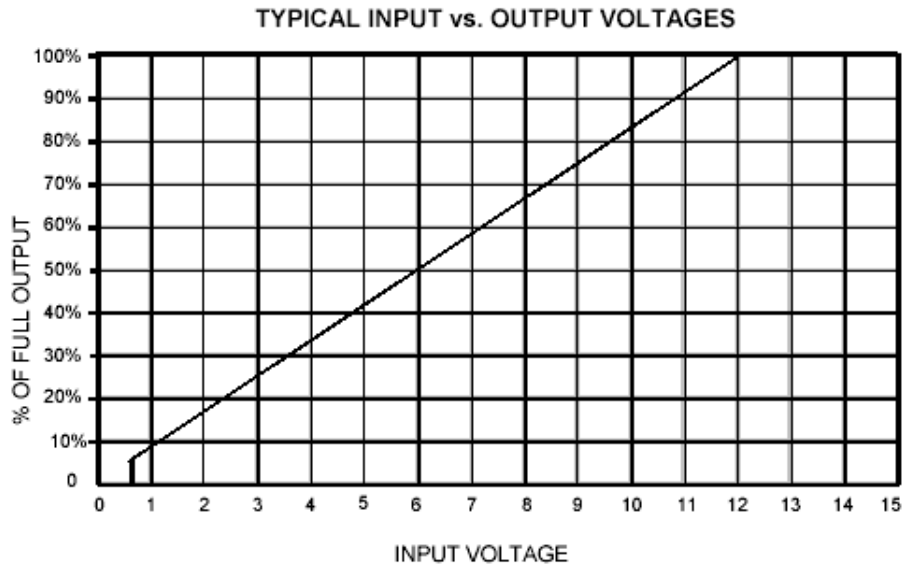
Figure 47. Input voltage versus percent output of HVDC ENCO G20 converter according to the manufacturer. Note the linear progression after 0.7V turn on. Taken from Ref. [50]

The HVDC converters function by converting the DC input to an AC signal, feeding this to a transformer which multiplies the voltage, and then converting back to a DC output signal with P-P ripple of less than 0.5% [50].

The output signals are supplied to the electron gun via a socket fitted with banana plug inputs. A Plexiglas board shown in Fig. 48 was used as opposed to epoxy circuit board, as it was feared that with the 2000V supplied at full load, discharges could occur between the terminals.

Figure 48. Photograph of HVDC converter Plexiglas mount board. Each HVDC converter powers a different section of the electron gun. Signal from the transistor amplifer is supplied via a ribbon cable. The HVDC connects to the electron gun via banana cables.

4.7 Microcontroller Code

The microcontroller is programmed in a form of BASIC known as PBASIC version 2.5. This is a dialect of BASIC that is designed to work with the BASIC stamp microcontroller. In order to make the language as small as possible, the number of commands available has been trimmed as much as possible.

The HV control code itself is included in Appendix B. The first two lines of code are a declaration of the type of language and the type of BASIC stamp. Next, the variables are declared, which store inputted values in memory, as well as the I/O pins to be used are activated. Pins 0-11 are used for the DAC digital data bus input, pins 12 and 13 are used for the multiplexing bits of the DAC, and pin 15 is used to turn the filament on and off. The next section sets the I/O pins to output mode as opposed to input mode. The subroutine OutputSet asks the user which element of the electron gun they wish to

modify: filament, horizontal deflection, focus, cathode, or intensity voltage. The 'a' character acts as a reminder of the need for a carriage return. Any non-number acts as a carriage return. Pauses are used to ensure that all components of the system have a chance to settle before any additional changes are made. Subroutines Sets 1-3 and 5 set the multiplexing bits on the DAC to the appropriate values for each register. Set 4 turns pin 15 on or off, which can be used to activate/deactivate the filament via a simple transistor circuit shown in Fig. 49.
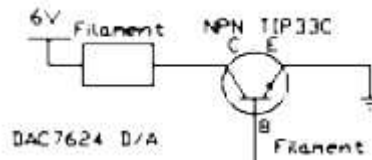
Figure 49. Schematic for filament circuit. Pin 15 from the microcontroller is fed into the base of the transistor.

Subroutine VoltageSet accepts a value from 0-4096, which covers the range of resolution of the DAC, and converts it from decimal form to binary. This section checks to see if it can subtract a power of two. If it can then it will activate the output pin that corresponds to that power of two, subtract that power of two from the user input, and will then move on to the next power. This is a simple algorithm to convert a decimal number to its binary equivalent. This binary equivalent is then output on the appropriate pins. The code will continue to loop back to asking which input wishes to be changed.

The code is burned onto the stamp's EEPROM via Parallax's BASIC Stamp Windows Editor 2.4. In order to do this, a direct serial connection is required. In order to communicate with the microcontroller once the fiber line is installed Windows

Hyperterminal is used with 9600 baud mode 8-N-1. Eventually, communicating with the

microcontroller could be done with LabVIEW over a GPIB bus, which would also allow

data to be collected from other devices on the GPIB bus, such as vacuum gauges, or

microammeters.

Chapter 5

CONCLUSIONS

5.1   Summary

The design history and current status of the Houghton College 200 keV electrostatic accelerator was described in this thesis. The current design uses an accelerating tube consisting of 48 high density polyethylene rings alternating with stainless steel washers compressed by nylon threaded rod. The electron gun is constructed from a RCA 3RP1 cathode ray tube, is powered by a high voltage amplifying circuit, and is controlled by a microcontroller which is mounted inside the high voltage terminal.

5.2   Current Results

The accelerator tube and electron gun have been constructed. The system was pumped down to a pressure of approximately 4×10^{-6} torr. With the accelerator tube removed and a test circuit attached a beam spot was observed. However, the electron gun appears to have not been mounted squarely, such that the electron beam line and the alignment of the mounting flange with respect to the accelerator axis are not parallel. Therefore, some voltage on the horizontal control grid is required to center the beam spot. The beam current appears to take a period of approximately half of an hour after filament activation to maximize, which may be due to water contaminating the cathode metal oxide layer converting it to a hydroxide, greatly increasing the value of the work function. However, upon baking a hydroxide at high temperature in a vacuum the hydroxide will be converted back to an oxide. This is may explain why the beam current seems to increase

after a period of minutes. However, the beam current is still small and the beam spot is strangely shaped, which may point to additional issues with the current electron gun.

The control circuit has been built and is able to control the voltage outputs of the HVDC converters. The Ethernet/GPIB section of the terminal interface has not been tested with the current setup but has been shown to function in independent tests. Testing of the linearity and stability of the circuit has not been completed. A beam spot has not been produced using the microcontroller circuit due to the difficulty in tuning all of the grids of the electron gun to the proper voltages simultaneously.

5.3   Future Plans

The accelerator is moving toward the ability to produce an electron beam of which the energy spectrum will be measured. However, issues with the electron gun and control circuit must first be rectified. Once a reliable beam spot is produced, the accelerator may be attached to the Van de Graaff generator, allowing it to generate at 200 keV beam of electrons. A scintillator can be mounted near the phosphorescent screen to measure bremsstrahlung X-ray radiation, so that the end point can be measured to determine the energy of the accelerator. Additionally, the beam current may be measured via a microammeter.

In addition there are several plans for the accelerator once the energy spectrum has been measured. First, the Ethernet/GPIB interface should be completed, perhaps even before measuring the energy spectrum. The GPIB interface would allow LabVIEW to interface

with the electron gun's microcontroller, in addition to other equipment such as pressure gauges, microammeter outputs, or even relays for powering on/off equipment.   In addition, a motor-generator set could be used to replace the batteries currently used to power the control circuit. It could consist of an electric motor mounted underneath the high voltage terminal, sufficiently far away as to avoid corona discharge, and have an insulating shaft penetrate into the high voltage terminal where it would be attached to a generator.   Finally, it is possible to upgrade the Van de Graaff generator to be able to provide increased current so that the potential will be higher. Ways to do this include: upgrading the motor to allow the belt to move faster, widening the belt, or spraying charge on to the belt to move charge from the high voltage terminal to base of the Van de Graaff generator.

Appendix A

Vacuum System

A.1   Introduction

In order to maximize the beam current by minimizing the number of interactions of accelerated particles with gas in the acceleration tube, a vacuum system is used shown in Figure 50. This particle accelerator typically achieves pressures on the order of 10^{-6} torr via the use of a Alcatel M2008A rotary forepump, a Kurt J. Lesker Company TLR6XS150QF liquid nitrogen filled cold trap, and a Varian 0159 diffusion pump. One Duniway Stockroom Corp. I-100-K iridium filament ion gauge is used at the top of the vacuum system for measuring pressures below 10^{-4} torr along with two Duniway Stockroom Corp. CVT-275-101 thermocouple convection gauges to measure the higher pressures; one for the foreline and one for the chamber. The lowest pressures recorded so far are $2.0\text{x}10^{-6}$ torr with the accelerator tube not attached and $4.9\text{x}10^{-6}$ torr with the accelerator tube attached. The system is connected with 1.5 inch stainless steel tubing with 2.75 inch Kwik-Flange or Conflat connections sealed with Viton gaskets.

A.2   Forepump

 The forepump is the first pump in the series and is responsible for generating the initial vacuum. This accelerator uses an Alcatel M2008A rotary forepump which is powered by a Franklin Electric 0.5 hp motor running at 1750 rpm.

This rotary pump is able to generate a vacuum of $6\text{-}8\text{x}10^{-3}$ torr. With each revolution of the pump the same volume of gas is removed. The gas is forced out by the turning of the vanes which are held to the pump housing by a spring as shown in Fig. 51.

Key

1. Ion Gauge
2. Thermocouple Vacuum Gauge
3. Electron Gun
4. Accelerator Tube
5. Ceramic Insulating Tube
6. Target
7. Butterfly Valve
8. Cold Trap
9. Diffusion Pump
10. Air Inlet Valve
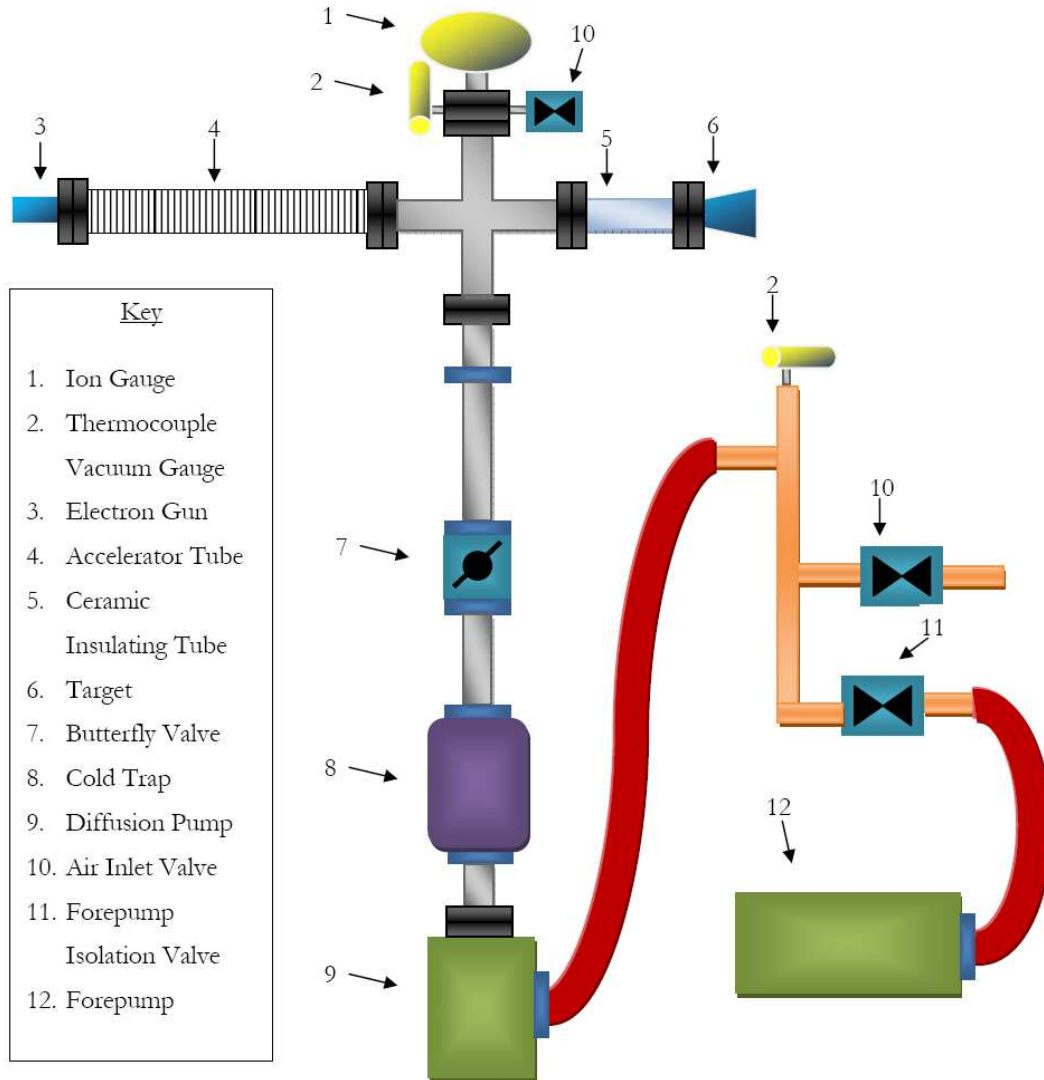11. Forepump Isolation Valve
12. Forepump

Figure 50. Drawing of the Vacuum System. All stainless steel tubes are shown in gray with Conflat flanges in black, quick flanges in blue, rubber tubing in red and copper pipes in orange. Taken from Ref. [46].
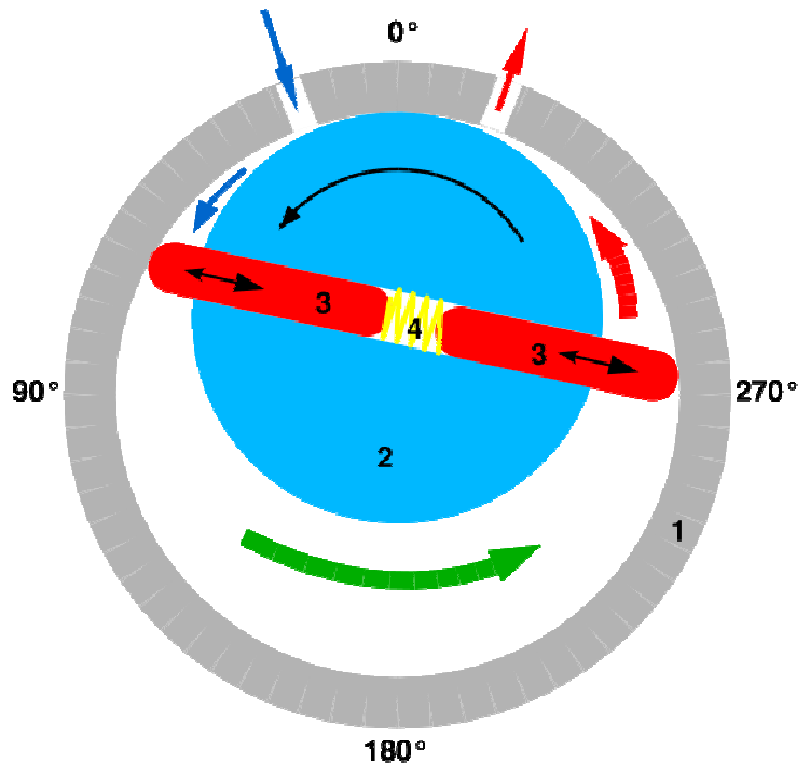
Figure 51-Diagram of Rotary Pump. Air from the system enters at the top left and leaves at the top right. 1 is the pump housing, 2 is the rotor, 3 are the vanes, and 4 is the spring that holds the vanes to the pump housing.

A.3 Diffusion Pump

The next stage in the vacuum system is a Varian 0159 diffusion pump. The diffusion pump sprays a jet of oil vapor downward toward its exhaust, which is connected to the inlet of the fore pump. As the oil vapor flows downward, remaining gas is brought with it and is eventually removed by the forepump. The vapor eventually condenses on the walls of the diffusion pump which are air cooled. Upon condensing, it is again boiled by a 350W heater and directed to the downward jet. This pump operates with 50cc of Dow Corning 704 silicone based diffusion pump oil. The diffusion pump is able to lower the

66

total pressure of the accelerator to 4.9×10^{-6} torr. The diffusion pump has no moving parts, as it operates by the pressure of the boiling oil. However, the diffusion pump cannot be turned on until a vacuum of $\sim 10^{-3}$ torr is obtained by the forepump or else the oil can scorch, contaminating the entire system. Upon startup, the diffusion pump will initially cause the pressure to rise before the oil is heated to operating temperature as contaminates are driven out of the oil.

A.4 Cold Trap

The final component in the vacuum system is a cold trap, which is a chamber that is cooled by liquid nitrogen at 77K. The cold trap causes many contaminants to condense and fall into the forepump. The cold trap is particularly effective at removing water vapor in addition to oil contamination from the other pumps. Also, the cold trap lowers the kinetic energy of all residual gas molecules in the system, again making it easier for the forepump to remove them. This vacuum system uses a Kurt J. Lesker Company TLR6XS150QF cold trap.

A.5 Gauges

The system is monitored by three vacuum gauges. Two gauges are convection type ConvecTech Gauge Tubes from Duniway Stockroom Corp. CVT-275-101. One is mounted at the top of the system, the other mounted in the foreline. They are able to measure pressure down to 10^{-3} torr. The third gauge is a Duniway Stockroom Corp. I-100-K iridium filament ion gauge. This gauge is able to measure pressures from 10^{-3} to 10^{-10} torr. The ion gauge operates by heating a filament to ionize any residual gas. The resulting current of ionized gas is proportional to the amount of residual gas in the system. However, if pressures are too high, the filament can be damaged. All gauges are

attached to a Stanford Research Systems IGC100 ion gauge controller which has digital

readouts, as well as a safety to keep the ion gauge from burning out due to too high of a

pressure. For the most accurate readings, the ion gauge should be allowed to reach

operating temperature for a few minutes.

Appendix B

The microcontroller code is written to convert a user entered voltage multiplier value to

binary bits. The first section of the code declares variables and sets the microcontrollers

I/O bus to output mode. The next section of code selects which of the 5 controllable

voltages is to be modified. Next is the code that converts the decimal voltage multiplier

to binary bits. The final subroutines select which channel of the DAC is to be selected.

Pauses are entered to allow voltages to settle.

Microcontroller Code

```
' {$STAMP BS2}
' {$PBASIC 2.5}


'Declare Variables

Pin2V VAR  Bit
Pin1V VAR  Bit
Fil   VAR  Bit
Out   VAR  Byte
Voltage VAR Word
Pin0  PIN  0
Pin1  PIN  1
Pin2  PIN  2
Pin3  PIN  3
Pin4  PIN  4
Pin5  PIN  5
Pin6  PIN  6
Pin7  PIN  7
Pin8  PIN  8
```

```
Pin9  PIN  9
Pin10 PIN  10
Pin11 PIN  11
Pin12 PIN  12
Pin13 PIN  13
Pin15 PIN  15


main:
'Set I/O Pins to Output
OUTPUT Pin0
OUTPUT Pin1
OUTPUT Pin2
OUTPUT Pin3
OUTPUT Pin4
OUTPUT Pin5
OUTPUT Pin6
OUTPUT Pin7
OUTPUT Pin8
OUTPUT Pin9
OUTPUT Pin10
OUTPUT Pin11
OUTPUT Pin12
OUTPUT Pin13
OUTPUT Pin15
GOSUB OutputSet



OutputSet:
SEROUT 16, 84, ["Enter control (1=Hor, 2=Foc, 3=Cat, 4=fil, 5=Cont) and press 'a'   "]
PAUSE 500
SERIN 16, 84, [DEC Out]
PAUSE 500
SEROUT 16, 84, ["You entered  ", DEC Out, "   "]
IF (Out = 1)THEN GOSUB Set1
IF (Out = 2)THEN GOSUB Set2
IF (OUT = 3)THEN GOSUB Set3
IF (OUT = 4)THEN GOSUB Set4
IF (OUT = 5)THEN GOSUB Set5
GOSUB OutputSet


VoltageSet:
SEROUT 16, 84, ["Enter voltage multiplier (0-4095) and press a "]
PAUSE 100
```

```
SERIN 16, 84, [DEC Voltage]
PAUSE 500
SEROUT 16, 84, ["You entered  ", DEC Voltage, "   "]
PAUSE 500
Pin13 = Pin1V
Pin12 = Pin2V
IF (Voltage >= 2048) THEN Pin11 = 1 ELSE Pin11 = 0
IF (Voltage >= 2048) THEN Voltage = Voltage - 2048
'Pin11 = Voltage.BIT11  'MSB
IF (Voltage >= 1024) THEN Pin10 = 1 ELSE Pin10 = 0
IF (Voltage >= 1024) THEN Voltage = Voltage - 1024
'Pin10 = Voltage.BIT10
IF (Voltage >= 512) THEN PIN9 = 1 ELSE PIN9 = 0
IF (Voltage >= 512) THEN Voltage = Voltage - 512
'Pin9 = Voltage.BIT9
IF (Voltage >= 256) THEN PIN0 = 1 ELSE PIN0=0
IF (Voltage >= 256) THEN Voltage = Voltage - 256
'Pin0 = Voltage.BIT8
IF (Voltage >= 128) THEN Pin1 = 1 ELSE Pin1=0
IF (Voltage >= 128) THEN Voltage = Voltage - 128
'Pin1 = Voltage.BIT7
IF (Voltage >= 64) THEN PIN2 = 1 ELSE PIN2=0
IF (Voltage >= 64) THEN Voltage = Voltage - 64
'Pin2 = Voltage.BIT6
IF (Voltage >= 32) THEN PIN3 = 1 ELSE PIN3=0
IF (Voltage >= 32) THEN Voltage = Voltage - 32
'Pin3 = Voltage.BIT5
IF (Voltage >= 16) THEN PIN4 = 1 ELSE PIN4=0
IF (Voltage >= 16) THEN Voltage = Voltage - 16
'Pin4 = Voltage.BIT4
IF (Voltage >= 8) THEN PIN5 = 1 ELSE PIN5=0
IF (Voltage >= 8) THEN Voltage = Voltage - 8
'Pin5 = Voltage.BIT3
IF (Voltage >= 4) THEN PIN6 = 1 ELSE PIN6=0
IF (Voltage >= 4) THEN Voltage = Voltage - 4
'Pin6 = Voltage.BIT2
IF (Voltage >= 2) THEN PIN7 = 1 ELSE PIN7=0
IF (Voltage >= 2) THEN Voltage = Voltage - 2
'Pin7 = Voltage.BIT1
IF (Voltage >= 1) THEN PIN8 = 1 ELSE PIN8=0
'IF (Voltage >= 1) THEN Voltage = Voltage - 1
'Pin8 = Voltage.BIT0
PAUSE 500
GOSUB OutputSet
```

```
Set1:
Pin1V = 0
Pin2V = 0
PAUSE 500
SEROUT 16, 84, ["Hor selected    "]
GOSUB VoltageSet

Set2:
Pin1V = 0
Pin2V = 1
PAUSE 500
SEROUT 16, 84, ["Focus selected    "]
GOSUB VoltageSet


Set3:
Pin1V = 1
Pin2V = 0
PAUSE 500
SEROUT 16, 84, ["Cathode selected    "]
GOSUB VoltageSet


Set5:
Pin1V = 1
Pin2V = 1
PAUSE 500
SEROUT 16, 84, ["Intensity selected    "]
GOSUB VoltageSet

Set4:
PAUSE 500
SEROUT 16, 84, ["Fil selected    "]
SEROUT 16, 84, ["Enter Filament Setting (0=Off, 1=On) and press 'a'    "]
PAUSE 100
SERIN 16, 84, [DEC Fil]
PAUSE 500
SEROUT 16, 84, ["You selected    ",  DEC Fil]
Pin15 = Fil
GOSUB OutputSet
```

References

_____

[1] H. W. Geiger and E. Marsden, *Proc. Roy. Soc.* **82**, 495 (1909).

[2] H. Geiger and E. Marsden, *Philos. Mag.* **27**, 604 (1913).

[3] James William Rohlf. **Modern Physics from a to Z0**,(Wiley, 1994)

[4] E. Rutherford, *The London, Edinburgh and Dublin Philosophical Magazine and Journal of Science*, 6th series, **37**: 581 (1919).

[5] G. Gamow, *Z. Physik,* **52,** 510 (1929).

[6] E Rutherford, *Proc. Roy. Soc. (London)* **A117**, 300 (1927).

[7] P. L. Bellaschi, *Trans. Am. Inst. Elec. Engrs.* **51***,* 936 (1932).

[8] A. Brasch and F. Lange, *Naturwiss.* **18***,* 769 (1930).

[9] A. Brasch and F. Lange, *Z. Physik* **70***,* 10 (1931).

[10] R. W. Sorenson, *J. Am. Inst. Elec. Engrs.* **44,** 373 (1925).

[11] R. Crane and C.C. Lauritsen. *Rev. Sci. Instr.* **4***,* 118 (1933).

[12] R. Crane and C.C. Lauritsen. *Phys. Rev.* **45,** 226 (1934).

[13] G. Breit, M.A. Tuve, and O.Dahl, *Phys. Rev*., **35,** 51 (1930).

[14] M.A. Tuve, G. Breit, and L.R. Hafstad, *Phys. Rev*., **35**, 66 (1930).

[15] M.A. Tuve, L.R. Hafstad, O. Dahl, *Phys. Rev*., **35,** 1406 (1930).

[16] M.A. Tuve, L.R. Hafstad, O. Dahl, *Phys. Rev*., **36**, 1261 (1930).

[17] D.H. Sloan, *Phys. Rev.,* **47,** 62 (1935).

[18] M. Livingston. **Particle Accelerators: A Brief History** (Harvard University Press, Cambridge, 1969).

[19] J.D. Cockroft and E.T.S Walton, *Proc. Roy. Soc*. (London) **A136,** 619(1932).

[20] J.D. Cockroft and E.T.S Walton, *Proc. Roy. Soc*. (London) **A137**, 229(1932).

[21] J.D. Cockroft and E.T.S Walton, *Proc. Roy. Soc*. (London) **A144**, 704 (1934).

[22] G. Gamow, *Nature,* **123,** 606 (1929).

[23] R.W. Gurney and E.U. Condon, *Phys. Rev.,* **33,** 127 (1929).

[24] G. W. Kaye *et al. Rep. Prog. Phys.* **6,** 95 (1939).

[25] R.J. Van de Graaff, *Phys. Rev*, **38**, 1919A (1931).

[26] R.J. Van de Graaff *et. al*., *Phys. Rev*., **49,** 761 (1936).

[27] R.J. Van de Graaff *et al., Rev. Sci. Instr.* **12,** 534 (1941).

[28] M.A. Tuve *et al.*, *Phys Rev.* **48,** 315 (1935).

[29] R.G. Herb *et al. Rev. Sci. Instr.* **6,** 261 (1935).

[30] R. G. Herb and E. J. Bernet, *Phys. Rev.,* **52**, 379 (1937).

[31] J. G. Trump *et al., Trans. AIEE,* **60**, (1950).

[32] R.G. Herb *et al. Phys Rev.* **53,** 642 (1938).

[33] R.G. Herb *et al. Phys Rev.* **58,** 579 (1940).

[34] J.G. Trump and R.J. Van de Graaff, *Phys Rev.* **55,** 1160 (1939).

[35] R.J. Van de Graaff, *Nuclear Instr. Methods,* **8**, 195 (1960).

[36] E. O. Lawrence and M. S. Livingston, *Phys. Rev*., **40,** 19 (1932).

[37] W. K. H. Panofsky and M. Breidenbach, *Rev. Mod. Phys.*, **72**, 121 (1999).

[38] C.L. Stong, *Scientific American*, **200**, 1, (1959)

[39] C.L. Stong, *Scientific American*, **225**, 2, (1971)

[40] "Fred's World of Science: Linear Accelerator" http://www.niell.org/linac.html. (June 25, 2008)

[41] F.W. Peek. **Dielectric Phenomena in High Voltage Engineering** (McGraw Hill, 1929).

[42] Radio Corp. of America, RCA 3RP1 (Data Sheet) (1949).

[43] "MA Lamp Electrodes"
http://www.lamptech.co.uk/Documents/M8G%20MA%20Electrodes.htm. (June 30, 2008)

[44] B. Winey, B.S. thesis, Houghton College, 2002.

[45] P. Brady, B.S. thesis, Houghton College, 2004.

[46] J. Troyer, B.S. Thesis, Houghton College, 2007.

[47] Parallax Inc., Basic Stamp Syntax and Reference Manual (Data Sheet).

[48] Burr-Brown Corp., DAC7625 (Data Sheet).

[49] "A digital DC powersupply"
http://www.tuxgraphics.org/electronics/200506/article379.shtml (June 11, 2007)

[50] EMCO High Voltage Corp., EMCO G20 (Data Sheet).